Enhancing Oncolytic Immunotherapy through Induction of Immunogenic Cell Death

Submitted by

Jiarun Wei

A thesis submitted to the School of Graduate Studies in partial fulfillment of the requirement for

the degree of Master of Science, Specialization in Biochemistry

McMaster University

Faculty of Health Science

Department of Biochemistry

Supervisor:

Karen Mossman

Supervisory Committee

Yonghong Wan

Jonathan Bramson

Abstract

Oncolytic viruses (OVs) are natural or engineered viruses that specifically infect and kill cancer cells without harming healthy tissues. Cancer cells killed by OV infection expose tumor antigens along with viral components and intracellular factors that mediate inflammation. Ideally, this process elicits an anti-tumor immune response that controls tumor growth. Herpes simplex virus type 1 (HSV-1) is a candidate OV that has proven therapeutic efficacy in preclinical cancer models. However, therapeutic efficacy of current oncolytic HSV-1 (oHSV-1) is limited in immunologically hot cancers such as melanoma. Here we showed that oHSV-1 expressing a modified B-box (HMB) of high mobility group box 1 (HMGB1), a potent ligand of toll-like receptor (TLR) 4-MD2, provides marginal therapeutic benefit in mice bearing breast cancer. Comparing with parental oHSV, tumor-bearing mice treated with oHSV-1-HMB showed improved survival and reduced tumor burden. Our results demonstrated the potential to improve oHSV-1 with immunogenic cell death modulators. We anticipate our oHSV-1-HMB to provide additive benefit with the combination of immunological checkpoint blockade.

Table of Contents

List of Abbreviations

APC	Antigen presenting cells		LPS	Lipopolysaccharide
ATP	Adenosine triphosphate		LRP1	Lipoprotein receptor-related protein 1
BHV	Bovine herpes virus		MHC	Major histocapacity complex
cGAS	Cyclic GMP-AMP synthase		NLS	Nuclear localization sequences
CRT	Calreticulin		oHSV	Oncolytic herpes simplex virus
CTLA-4	Cytotoxic T lymphocyte associated protein 4		OV	Oncolytic virus
DAMP	Damage associated molecular pattern		PAMP	Pathogen-associated molecular pattern
DC	Dendritic cells		PD-1	Programmed death 1
eIF	Eukaryotic initiation factor		PKR	Protein kinase R
ER	Endoplasmic reticulum		PRR	Pattern recognition receptors
GMCSF	granulocyte-macrophage colony stimulating factor		RAGE	Receptor for advanced glycol end product
HER2	Human epithelial growth factor receptor 2		STING	Stimulator of interferon genes
HMB	B-box of HMGB1		TAA	Tumor associated antigen
HMGB1	High mobility group box 1		Tcf	Wnt/b-catenin/T-cell factor
HVEM	Herpes virus entry mediator		TCR	T cell receptor
ICB	Immunological checkpoint blockade		TGF	Transforming growth factor
ICP	Infected cell protein		TLR	Toll-like receptor
IFN	Interferon		TNF	Tumor necrosis factor
IL	Interleukin		TVEC	Talimogene Laherparepvec
IRF	Interferon regulatory factor		UTR	Untranslated region
ISG	Interferon stimulated gene		VSV	Vesicular stomatitis virus

1. Introduction

1.1 Challenges to Cancer Immunotherapy

Cancer immunotherapies are targeted cancer treatments that control cancer through the establishment of adaptive immune responses against cancer cells. Compared to traditional cancer therapies, immunotherapies are often less toxic, effective against distal metastasis, and can be durable after treatment ceased. Over the past decade, several types of cancer immunotherapeutics have demonstrated improved efficacy over traditional therapies and have become available for routine clinical management. These include immunological checkpoint blockade (ICB) therapies that alleviate T cell suppression by interfering with signalling through programmed death (PD)-1 or cytotoxic T lymphocyte-associated protein (CTLA)-4[1]; and oHSV-1 expressing granulocyte-macrophage colony-stimulating factor (GMCSF) (Talimogene Laherparepvec, TVEC)[2]. However, the benefit of cancer immunotherapy is largely limited in immunologically hot cancers with high mutational load and tumor-infiltrating lymphocytes. ICB as a stand-alone treatment elicits durable tumor-targeting T cell response and improved disease outcome in significant portions of patients with non-small cell lung carcinoma (20%)[3,4], renal carcinoma (22-25%)[5] or melanoma (31-44%)[6]. However, ICB is much less effective in immunologically cold cancers such as breast or pancreatic cancers. TVEC provides clinical efficacy in treating melanoma[2], but not in head and neck carcinoma[7] or pancreatic cancer[8]. The establishment of a protective anti-tumor immune response has three major requirements: recognition of tumor antigens through the T cell receptor, a co-stimulatory signal from activated antigen presenting cells, and homing and infiltration of activated T cells to tumors. Likewise, a challenge to cancer immunotherapy revolves around these three aspects. First, as cancers originate from host cells, most cancer cell antigens are tolerized through central or peripheral tolerance and immune-mediated cancer

clearance relies on a T cell repertoire that targets tumor specific neoantigens. Therefore, it is challenging to raise effective anti-tumor immunity in cancers with low rates of somatic mutation[9,10]. The other challenge comes from tumor microenvironments that resist immune clearance. These include overexpression of surface molecules that induce effector T cell exhaustion and recruitment of immune-regulatory cells[1]. In practice, both of these challenges contribute to the limited efficacy of immunotherapy.

Tumors originate from healthy cells acquiring genomic alterations that enable indefinite and uncontrolled cell division. These mutations generate neoantigens that differentiate cancer cells from non-cancerous counter parts. Neoantigens are generated from four origins: over-expressed somatic proteins, such as mitogen receptors[11] or proteins that amplify downstream signalling[12]; mutated somatic proteins, including disabled growth inhibitors and tumor suppressor[13]; germ-line proteins, such as transcriptional regulators that function in male germ-line cells or during embryonic development[14]; and viral proteins in oncovirus-driven cancers. In addition to driver mutations, cancer cells also harbour passenger mutations that result from genomic instability[9]. Protective adaptive immune responses specific towards cancer cells require T cells targeting these neoantigens. Tumor mutational burden is a quantitative measurement of mutation frequency in cancer cell genome. Cancers with low mutational burden, which correlate to limited neoantigens, are less likely to respond to cancer immunotherapy[15,16]. Drug inhibition of epigenetic silencing, such as DNA methylation and histone deacetylation, has been shown to increase the expression of tumor antigens in cancers with low mutational burden[17–19]. Therefore epigenetic modulating drugs can be combined with other forms of immunotherapy to improve efficacy.

Another major challenge to cancer immunotherapy is immunosuppression in the tumor microenvironment. Establishment of an anti-tumor immune response requires activated antigen presenting cells (APC) to sample tumor antigens from tumors and prime antigen specific T cells in the lymph node. Certain lineages of dendritic cells (DCs) such as plasmacytoid DCs are particularly efficient in stimulating anti-tumor cytotoxic T cells[20] due to their ability to cross-present engulfed antigen onto MHC class I. T cell priming requires the recognition of tumor antigens presented from mature APC by T cell receptors (TCR) (signal 1), and co-stimulatory signals (signal 2). DC maturation characterized by the expression of 4-1BBL, B7, OX40L requires detection of danger signals in the environment. These include microbial components known as pathogen associated molecule patterns (PAMPs) and intrinsic cellular factors known as damage associated molecular patterns (DAMPs). These danger signals engage pattern recognition receptors (PRR) on APCs, leading to recruitment of these APCs, NF-κB activation, up-regulation of co-stimulatory molecules, and production of cytokines that are essential in establishing T cell responses. Tumors with low levels of DAMPs, or an abundance of immunosuppressive cytokines such as transforming growth factor (TGF) beta are correlated with defective recruitment of APCs and an absence of T cell co-stimulation[21]. ICD, which is characterized by cell surface presentation of calreticulin (CRT) or release of heat shock proteins, HMGB1 and ATP, is an important source of both tumor antigens and DAMPs. One example of cancer cell-mediated immunosuppression is through overexpression of CD73, a cell surface-bound nucleotidase that dephosphorylates ATP, a potent chemoattractant of DCs, into adenosine, which inhibits DC maturation[22]. Radiotherapy and chemotherapy drugs that promote cancer cell ICD are correlated with a higher abundance of tumor antigen specific T cells[23,24]. Another method to circumvent cancer-induced immunosuppression is the use of oncolytic viruses, which

uses natural or engineered viruses that preferentially infect cancer cells. Both the engagement of interferon responses by viral components and the release of viral PAMPs are potent stimulators to DC maturation.

1.2 Oncolytic immunotherapy

Oncolytic immunotherapy is an emerging form of cancer immunotherapy that utilizes replication-competent viruses to elicit anti-tumor immune responses. To date, one strain of oHSV expressing GM-CSF, known as T-VEC, has been approved by the FDA to treat melanoma, OVs derived from other virus species, including vaccinia, vesicular stomatitis virus, adenovirus, have exhibited therapeutic efficacy in both preclinical models and clinical trials. The efficacy of oncolytic immunotherapy is mediated through two mechanisms: direct lysis of infected tumor cells, and initiation of cytotoxic immune responses against tumor cells. OVs can be used in its wild-type strains or genetically modified to remove virulence factors, ensure tumor specific infection, and enhance immune stimulation. In this section of introduction, the mechanism of oncolytic immunotherapy is reviewed with focus on oHSV and engineering strategies to overcome current challenges.

1.2.1 Tumor-selective infection

Specific targeting of cancer cells is required for oncolytic viruses to ensure safety and therapeutic efficacy. This can be achieved by limiting either entry or replication of oncolytic virus to cancer cells. Susceptibility of cells to a certain virus is defined by the presence of surface receptors that can bind to viral surface proteins that regulate attachment and entry. For instance, attachment of HSV onto host cells is mediated by the binding of glycoproteins gB and gC to

heparan sulfate proteoglycan, and binding of gD to herpes virus entry mediator (HVEM) or nectin-1. Entry is mediated by the interaction between viral glycoprotein gH/gL and alpha v beta 3 integrin. OVs can be engineered to recognize surface molecules abnormally over-expressed on cancer cells for viral entry. Human epithelial growth factor receptor 2 (HER2) is overexpressed in 25 to 30 percent of breast cancer patients[25]. By fusing gB or gH with single-chain antibody targeting HER2 and by deleting gD, infection by HSV can be retargeted and restricted to cancer cells with HER2 overexpression[26,27].

Another method to ensure tumor-specific replication of OVs is to genetically modify essential viral gene so they are expressed only in cancer cells. For instance, eukaryotic initiation factor (eIF) 4e, which forms part of the translational initiation complex eIF4F, is responsible for resolving secondary structures in the 5' untranslated region of mRNAs. eIF4E is overexpressed in a variety of cancers[28]. A prostate cancer-restricted oHSV was constructed by placing infected cell protein (ICP) 27, an essential viral gene, under the prostate-specific promoter and adding a secondary structure sequence in its 5' untranslated region (UTR). So oHSV replication is only restricted in prostate cancer cells[29]. A similar approach in constructing oHSV in which the essential viral gene ICP4 is placed under the Wnt/b-catenin/T-cell factor (Tcf) responsive elements also provided safe and effective response in pre-clinical tumor model[30].

Oncolytic viruses are also engineered to take advantage of the dampened anti-viral response in cancer cells. Healthy cells have a variety of sensors that can recognize viral components[31,32] and activate anti-viral responses. For instance, mRNA transcribed from HSV genes contain complementary sequences that form dsRNA. This activates dsRNA-dependent protein kinase (PKR)[33], which restricts viral replication by globally arresting mRNA translation. HSV evades PKR-mediated host translational arrest through the function of ICP34.5[34]. PKR is downregulated

in a variety of Ras-transformed caners[35]. One of the early oHSVs was made by ICP34.5 deletion as its replication is restricted in tumor cells[36]. In addition to cellular changes, many cancers also manipulate the tumor microenvironment to suppress immune effector function. While resisting immune effector function is a necessary process to allow cancer development, immune dysfunction in tumors also allows efficient viral infection in tumors. In healthy tissues, viral infection triggers the release of type I interferons, which stimulates an anti-viral state in neighboring cells and activates innate immune cells including NK cells, macrophages, and DCs to launch a coordinated anti-viral response. However, many cancer cells exhibit dampened interferon signalling[37] and tumor associated immune cells have reduced response to type I interferon[38]. HSV ICP0 is a multifunctional immune evasion factor expressed in the immediate early phase of HSV infection. It prevents interferon production by blocking the activation of interferon regulatory factor (IRF) 3 and IRF7, and through its E3 ubiquitin ligase activity, targets several interferon stimulated gene (ISG) products to degradation[39,40]. HSV with ICP0 deletion is significantly attenuated in tissue with intact interferon responses but not in human osteosarcoma cell lines[41] or preclinical breast cancer models[42]. ICP0-null oHSVs have exhibited significant therapeutic efficacy in pre-clinical breast cancer models[43,44].

1.2.2 Stimulation of anti-tumor immune responses

Induction of anti-tumor immune responses is a decisive factor to successful oncolytic immunotherapy. OVs not only carry viral PAMPs, but also induce immunogenic cancer cell death and can be engineered to express immunostimulatory cytokines that propagate anti-tumor immune responses. Priming of tumor antigen-specific T cells requires DCs to present TAAs with co-stimulatory signals. Cancer cells dying from OV infection provide such condition as they

expose TAAs to APCs in the context of activation signals. DCs acquire TAAs from the debris of tumor cells killed by OVs. DC maturation is stimulated by recognition of PAMPs or DAMPs by TLRs and by interferon signalling. For instance, in the presence of DNA virus replication, viral DNA leaking into the cytosol is recognized by cyclic GMP-AMP synthase (cGAS) and triggers production of cyclic GMP-AMP (cGMP-AMP). cGMP-AMP binds and activates stimulator of interferon genes (STING), which is a downstream signaling adaptor that stimulates the production of type-1 IFN through activation of IRF3 and NF-κB. STING is expressed in a variety of epithelial cells and immune cells including APCs such as macrophages and DCs. Activation of cGAS-STING in tumor-residing APCs is associated with improved response in a variety of cancers[45]. It is logical to hypothesize that with the abundance of both TAAs and viral PAMPs increasing proportionally with the degree of OV infection, enhancing intratumoral infection would improve oncolytic immunotherapy. This is true for oncolytic VSV as combination with a small-molecule viral sensitizer improves its efficacy in a preclinical melanoma model[46]. However, the degree of intratumor infection may not be the limiting factor for other OVs. In a preclinical breast tumor model, oHSV-1, which produced lower infectious units in the tumor and was cleared faster than its oHSV-2 counterpart, provided better response[44]. Rather, the improved efficacy of oHSV-1 was associated with higher levels of serum HMGB1 and heat shock proteins, which are molecular signatures of immunogenic cancer cell death.

1.2.3 ICD

ICD is a term to describe cellular demise accompanied with spatiotemporal release of DAMPs that stimulate immune responses against cellular antigens[21]. Cell surface calreticulin (ecto-CRT), extracellular ATP and HMGB1 are three important mediators of ICD. In brief, ATP leaked from

dying cells attracts innate immune cells including APCs to sites of ICD. Ecto-CRT on the surface of dying cells and cell debris sends "eat-me" signal to APCs to stimulate the engulfment of cell debris. HMGB1 stimulates local inflammation, enhances antigen processing by DCs, and promote DC maturation. OVs can trigger ICD through exerting stress on the endoplasmic reticulum (ER)[21] and engagement of interferon responses[47]. DAMPs released from ICD can potentially augment OVs in triggering anti-tumor immune responses.

ER stress is a common trigger of ICD which can be caused by OV infection or by ICD-inducing chemotherapies[21]. ER stress is caused by high levels of nascent peptides that exceed the folding capacity of the ER. During lytic infection, viral factors maximally exploit cellular machinery to construct progeny viruses, which creates a surge in protein synthesis and results in ER stress. The combination of therapies that cause Ca^{2+} efflux, and accumulation of reactive oxygen species in the ER, lead to the export and cell surface presentation of CRT in the early phase of ICD[24]. Ecto-CRT complexes with ERp57 during export from the ER, which then docks on CD91/low-density lipoprotein receptor-related protein 1 (LRP1). Ecto-CRT/ERp57 signals through CD91 and scavenger receptors on macrophages and DCs to promote phagocytosis of dying cells. The "eat-me" signal transduced by ecto-CRT can be antagonized by CD47, which transduces a "don't eat me" signal. CD47 is overexpressed by a large panel of solid and hematopoietic tumors[48] as a potential mean to resist phagocytosis. Antibody blockade of CD47 signalling contributes to tumor regression in some models[49]. These observations indicate the potential to improve cancer immunotherapy through enhancing tumor cell phagocytosis by APCs.

ATP donates high-energy phosphates to many cellular reactions. When released from apoptotic cells, extracellular ATP is a chemoattractant of monocytes and is sensed by P_2Y_2 receptors[50] on monocytes. Extracellular ATP also promotes inflammasome formation in DCs

through engaging purinergic P_2X_7 receptors, driving IL-1β secretion and induction of adaptive anti-tumor responses[51]. Various chemotherapies induce the release of ATP from treated tumors, and the extracellular ATP is shown to be required for chemotherapy-induced anticancer immunity[52]. The release of ATP is regulated by multiple pathways depending on the stage of apoptosis. ATP release at pre-apoptotic stages is mediated through classical and PERK-regulated proximal secretory pathways and PI3K-dependent exocytosis[53]. At the early phase of apoptosis, ATP release is dependent on autophagy[54]. Without continuous secretion, the immunostimulatory effect of extracellular ATP is transient as it is rapidly hydrolyzed by CD39 into adenosine monophosphate (AMP)[55] and then by CD73 into adenosine[22]. Adenosine suppresses CD8^{+} T cells and natural killer cells in turns of IFN gamma production and cytotoxicity. AMP also induces T cell anergy and recruits regulatory T cell. Both CD39 and CD73 can be overexpressed on tumor surfaces to prevent immune stimulation by ATP and to promote immune tolerance.
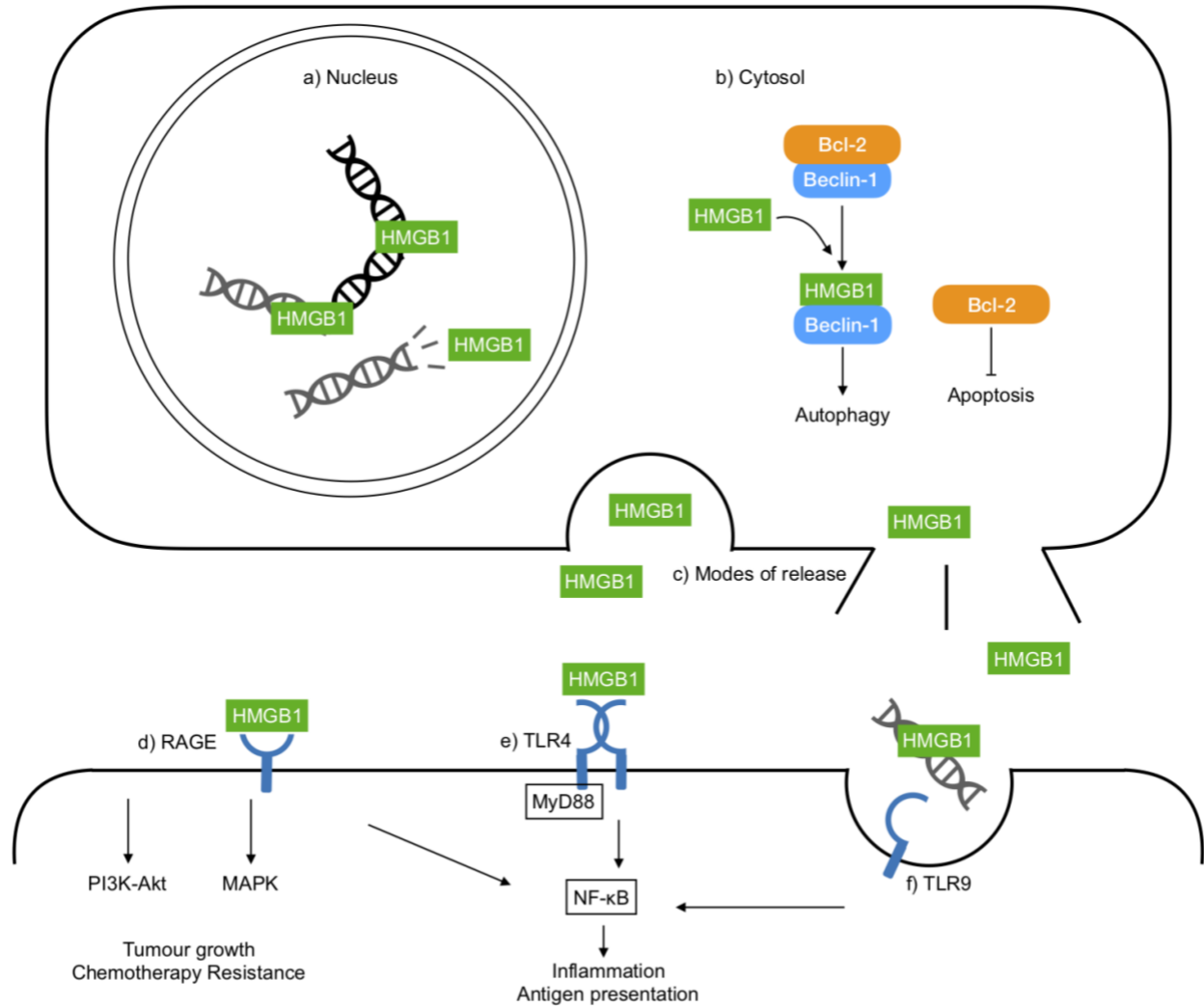
Figure 1: Function of HMGB1 in different compartments. a) In the nucleus, HMGB1 serves as a DNA chaperone. b) In cytosol, HMGB1 regulates autophagy through interaction with Beclin-1. c) Activated macrophage and neutrophils, and some colon cancer cells release HMGB1 through exocytosis. HMGB1 can also be released from damaged cells. d-f) HMGB1 engage various receptors on innate immune cells and cancer cells. d) RAGE signalling on cancer cells activate PI3K-Akt, MAPK. e) HMGB1 directly activate TLR4-MD2 complex. f) HMGB1 forms complex with extracellular nucleic acid and facilitate its endocytosis, which activates TLR9. RAGE, TLR4, and TLR9 signalling all activate NF-κB in innate immune cells, which induce inflammation. TLR4 signalling on DC may induce maturation and enhance antigen presentation.

Redox Forms	Source	Binding Partners	Functions
SH SH SH A-box — B-box — All-Reduced	Nucleus Cytosol Necrosis	DNA CXCL12 RAGE	- Bind DNA - Recruit immune cells - Inflammation
S—S SH A-box — B-box — Di-sulfide	Nucleus Cytosol Necrosis	DNA Beclin-1 TLR4 RAGE	- DNA chaperone - Induce Autophagy - Inflammation
S—S SO$_3$ A-box — B-box — Partially oxidized	Cytosol Apoptosis	RAGE?	- Inflammation?
SO$_3$ SO$_3$ SO$_3$ A-box — B-box — Fully oxidized	Apoptosis	No binding partner	Unknown
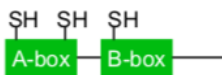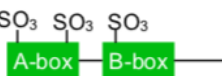
Table 1: Observed redox forms of HMGB1 and their functions. All-reduced and di-sulfide HMGB1 are predominant redox states observed in cells at resting states. These two forms are interchangeable. Partially or fully oxidized HMGB1 are produced as a result of ROS oxidation during caspase-mediated apoptosis. Structural of HMGB1-RAGE interaction has not been fully elucidated so whether partially oxidized HMGB1 can stimulate RAGE signalling is questionable.

1.3 Pleotropic role of HMGB1 in cancer

Another important marker of ICD is the release of extracellular HMGB1. HMGB1 is a multi-functional protein involved in diverse cellular activities. HMGB1 predominantly resides in the nucleus where it serves as a DNA chaperone to mediate protein interaction with DNA. It participates in transcriptional regulation, DNA damage responses, and maintenance of genome stability. It was later discovered that depending on its post-translational regulations and cellular condition, HMGB1 may translocate into the cytosol, onto cell membrane and outside of cells, where it regulates autophagy, cell signalling, and inflammation, respectively. HMGB1 is involved in aspects of cancer development. On one hand, its ability to maintain genomic stability and initiate autophagy maintains cellular homeostasis and suppress cell transformation, yet cancer cells also exploit these cellular function of HMGB1 to establish resistance to chemotherapies. Although in many established tumors, high level of intratumoral HMGB1 sustain inflammation and recruits innate immune cells that supports tumor growth; HMGB1 is also an important mediator to establish anti-tumor immune response. More detailed structural-functional characterization of HMGB1 is also revealing more interaction partners and adding dimensions to its role in cancer. Many agreed the influence of HMGB1 in immunotherapy is highly context dependent upon its post-translational modifications, the cellular compartment of which it is residing, the composition and activation status of the infiltrated immune cells in the microenvironment and the types of treatment used. Here, we review current understanding in the roles of HMGB1 in cancer development and various immunotherapies.

1.3.1 Nuclear functions of HMGB1

Nuclear functions of HMGB1 revolve around its interaction with genomic DNA. As HMGB1 is constantly present in the nucleus and binds DNA without sequence specificity, its activity is regulated through interaction with other DNA binding proteins[56]. HMGB1 binds DNA through minor grove interactions that bend the double helix. DNA bending is involved in regulating nucleosome structure, nucleosome sliding[57], and transcription. HMGB1 knockout mice develop lethal hypoglycemia shortly after birth due to defects in glucocorticoid receptor-mediated transcriptional regulation[58]. HMGB1 is also involved in DNA repair mechanisms given its ability to bind various DNA lesions. It participates in nucleotide excision repair, mismatch repair, and facilitates non-homologous end joining. Knockout or knockdown of HMGB1 significantly impairs the ability of cells to restore genomic integrity in response to oxidative stress, radiation, and chemotherapies[59,60].

1.3.2 Cytosolic function of HMGB1

In most cells at resting state, 90-95% of HMGB1 resides in the nucleus[57]. HMGB1 contains two lysine rich nuclear localization sequences (NLS). One NLS is embedded within the A box and the other is encoded on the C terminal tail. Acetylation of the lysine residues within the NLS abrogates its interaction with nuclear importin, allowing nuclear export. Cytosolic HMGB1 releases Beclin-1, a central regulator for autophagy, from sequestration by Bcl-2[61]. In most cells, cytosolic translocation of HMGB1 is upregulated in conditions that promote autophagy such as starvation or treatment with rapamycin or peroxide[61]. Depletion of cytosolic HMGB1 through gene silencing, RNAi or nuclear sequestration in human and mouse cancer cell lines significantly reduced autophagosome formation when treated with the same autophagy inducers[61].

1.3.3 Extracellular function of HMGB1

Outside of cells, HMGB1 can engage a variety of receptors and promote inflammation. HMGB1 is considered a damage associated molecular pattern as it alerts local immune cells when it passively leaks from cells undergoing necrosis. In the presence of bacterial infection, macrophages, and neutrophils actively release HMGB1 as part of their response to LPS and interferons[62]. High level of serum HMGB1 is responsible for sepsis or ischemia-induced shock[63–65], and treatment using HMGB1 antibody is effective against many inflammatory conditions[66]. Extracellular HMGB1 activates innate immune cells through receptor for advanced glycan endproduct (RAGE) and toll-like receptor (TLR4), and assists nucleic acid sensing through TLR9. HMGB1 also facilitates CXCL12 mediated chemotaxis. Serum HMGB1 enhances binding affinity between RAGE (expressed by monocytes and neutrophils) and Mac-1 integrin (expressed by activated endothelial cells), promoting leucocyte extravasation towards inflamed tissues. Interstitial HMGB1 recruits immune cells by signalling through chemokine receptor CXCL12. TLR signalling by HMGB1 up-regulate macrophage secretion of tumor necrosis factor (TNF), interleukin (IL)-6, and IL-1[65]. In general, extracellular HMGB1's pro-inflammatory activities were considered oncogenic, for the level of both serum and intratumoral HMBG1 are elevated in many cancer patients, and inflammation was one of the hallmarks in cancer development[67]. However, these complex signalling networks are highly influenced by the presence of other cytokines and the composition of immune cells. The engagement of HMGB1 with RAGE and TLR's provides maturation and migration signal to dendritic cells, which is a crucial step towards establishment of an anti-tumor immune response.

1.3.4 Post-transcriptional modification and regulation

HMGB1 is subjected to post-translational modifications including methylation, ADP-ribosylation, acetylation, phosphorylation, and oxidation[68]. These modifications regulate its binding affinities to DNA and proteins, which in turn influence its intracellular localization and function. In addition to acetylation[69], cytosolic translocation of HMGB1 can also be regulated by methylation[70] and phosphorylation[71]. The cytosolic and extracellular functions of HMGB1 are tightly controlled by redox states of its cysteine residues. HMGB1 has three cysteine residues, two in the A box at position 23 and 45, and the other in the B box at position 106 (thereafter referred to as C23, C45, and C106, respectively). Four oxidation states are observed and characterized for their chemokine/cytokine activity. Ranking by the level of oxidation, all-reduced HMGB1 (all three cysteine residues remain thiol side chains) possesses only chemokine function as this form binds CXCL12 with high affinity while it is unable to interact with TLR4. Disulfide HMGB1 (C23 and C45 form an intra-molecular disulfide bridge and C106 remain a thiol side chain) is the pro-inflammatory cytokine as it is the only form capable of activating the TLR4-MD2 complex. In the cytosol, only disulfide HMGB1 can interact with Beclin-2 and regulate autophagy. Partially oxidized (C23 and C45 form an intra-cellular disulfide bridge and C106 oxidized into a sulfonyl side chain), or fully-oxidized HMGB1 (all three cysteines oxidized into sulfonyl side chains) has no chemokine or cytokine activity. The redox state of extracellular HMGB1 is one of the fundamental features that differentiates immunogenic and non-immunogenic forms of cell death[68]. In resting cells, HMGB1 is maintained in the all-reduced or disulfide state, so the forms released from necrotic cells retain their chemoattractant or pro-inflammatory activity[72]. In cells undergoing apoptosis, caspase activation leads to production of reactive oxygen species from mitochondria, which oxidizes HMGB1 and prevents immune

activation[73]. Scientists are still investigating mechanisms that regulate other post-translational modifications and the biochemical characterization of interaction between these redox form and receptors in addition to TLR4.

1.3.5 HMGB1 is associated with tumorigenesis

Elevated levels of HMGB1 are observed in patients across a variety of cancer types and in pre-clinical models. HMGB1 is expressed at high levels in the B16 melanoma model[74]. In patients with colorectal cancer, tumors express HMGB1 at a significantly higher level than the surrounding, non-malignant tissue. The level of serum HMGB1 is significantly higher in patients with colorectal cancer than in healthy individuals, and patients with multiple metastases have an even higher level of serum HMGB1 than patients with localized tumors[75]. As extracellular HMGB1 can mediate inflammation, these observations are consistent with the role of chronic inflammation in promoting neoplastic transformation and tumor development[67]. In a murine colon cancer model, high levels of HMGB1 are shown to induce apoptosis in peritoneal macrophage-derived dendritic cells[76].

1.3.6 RAGE signalling

Among HMGB1's cognate receptors, signals downstream of RAGE have the most pro-tumor implications[77]. RAGE is a transmembrane receptor expressed on cancer cells, and innate immune cells such as neutrophils, macrophages, dendritic cells, vascular endothelial cells[77–79]. RAGE expression strongly correlates with the invasiveness and metastasis of colorectal[80] and gastric cancers[81]. Elevated incidences of cancer were observed in populations carrying RAGE with a G82S mutation which enhances its ligand binding and down-stream signal transduction[78,82].

HMGB1 secreted by alveolar macrophages is a main contributor to asbestos-induced mesothelial cell transformation, and antibody neutralization of extracellular HMGB1 or blockade of RAGE signalling decelerate mesothelioma formation[83]. Several mechanisms underlie the correlation between RAGE signalling and tumorigenesis. Engagement of RAGE on cancer cells is linked to activation of pro-survival and growth signals mediated through mitogen-activated protein kinases (MAPKs), PI3K/Akt, Rho GTPase, JAK/Stat, and Src family kinase activation[84]. Engagement of RAGE on innate immune cells activates Nuclear factor (NF)-κB. This central regulator increases transcription of pro-inflammatory cytokines[79], matrix metalloproteinases, and RAGE receptors[85]. These factors sustain an inflammatory tumor microenvironment and aid neoplastic growth and metastasis. In addition to promoting tumorigenesis, HMGB1 activation of RAGE underlies oxaliplatin resistance in colon cancers through its downstream signal that regulates mitochondrial fission[86]. Pre-treatment of oxaliplatin-resistant colon cancer cells with HMGB1 or RAGE-blocking antibodies restores their sensitivity to oxaliplatin.

1.3.7 Role of HMGB1 in anti-cancer immunity

Although HMGB1-mediated inflammation promotes tumorigenesis in many aspects, it contributes to the establishment of anti-tumor immune responses through its role in ICD. Central to HMGB1's role in ICD is the engagement of TLR4 which transmits activation signals to macrophages and DCs through the adaptor molecule MyD88[23]. Oxidation of C106 in HMGB1, which prevents its interaction with TLR4, is a necessary step during apoptosis to prevent allogenic immune activation[73]. Chemical sequestration of HMGB1 release or antibody neutralization diminished the immunogenicity of irradiated cancer cells[23]. Murine DCs lacking TLR4 or MyD88, but not other TLRs, failed to maturate in response to irradiated cancer cells or

to stimulate cytotoxic T cells. Tumor antigen specific CD8+ T lymphocytes are the fundamental force in immune-mediated tumor clearance. Priming CD8+ T cells requires mature DCs with tumor antigen presented on MHC class-I molecules. HMGB1-TLR4 signalling on DCs not only promotes maturation, but also cross-presentation of engulfed tumor antigens on MHC class I molecules, making them capable of priming CD8+ T cells. In addition to direct signalling, the ability for HMGB1 to aid detection of extracellular nucleic acid also promotes anti-tumor immune responses. A complex formed by extracellular nucleic acid, HMGB1 and uric acid facilitates the endocytosis of extracellular nucleic acid by dendritic cells and macrophages, leading to detection by TLR-9 and other nucleic acid sensors[87]. Established tumors evade macrophage engulfment through surface presentation of CD47, which sends "don't eat me" signal to phagocytes, and through programing tumor-associated macrophages into a non-phagocytic, pro-angiogenic phenotype. TLR9 signalling in tumor-associated macrophages restores their phagocytic ability and overrides CD47-mediated evasion. In addition to its direct signalling, HMGB1 also contributes to ICD through the induction of autophagy, which releases ATP. However, tumors can evolve mechanisms to selectively inhibit the HMGB1 from participating in the establishment of anti-tumor immunity. Surface receptor TIM-3 does so through impeding HMGB1 binding with extracellular nucleic acid, therefore inhibit HMGB1 mediated endocytosis of extracellular nucleic acid which can lead to TLR3, 7, 9 activation[74]. Surface expression of TIM-3 is elevated in DC infiltrated into established non-small cell lung cancer and breast cancers.

1.3.8 HMGB1 as a therapeutic target

Several studies have evaluated HMGB1 blockade as a cancer therapy. Treatment with soluble RAGE decelerates the growth of implanted glioma in SCID mice[88]. In a colon cancer liver metastasis model using immunocompetent mice, ethyl pyruvate-inhibition of HMGB1 reduces hepatic tumor growth in a dose-dependent manner[89] although this is accompanied by reduced immune infiltrate from all lineages. Further studies are necessary to decipher signalling pathways (or the lack of) responsible for these observations, and evaluate how HMGB1 blockade affects anti-tumor immune responses. Immunological checkpoint blockade is a clinically successful therapy to override tumor-mediated immune suppression. Supplementation of HMGB1 may improve the response to current checkpoint blockade therapies. In lung cancer and breast cancer models, blockade of TIM3, one of the immunological checkpoint molecules, failed to improve DC inflammatory responses towards dying tumor cells in presence of HMGB1 antibody[74].

1.4 Rational and Hypothesis

HSV-1 possesses many inherent oncolytic properties, making it a versatile template to be engineered into an immunotherapeutic[90]. However, its use in immunologically cold tumors such as breast cancers is still limited. Our research group seeks to identify factors that improve the therapeutic efficacy of oHSV in breast cancer models. By comparing two similar strains of oHSV in a tolerized breast tumour model, our group showed that the efficacy of oHSV is correlated with the induction of ICD[44]. Efficacy of oHSV could be further improved when combined with the immunogenic chemotherapy mitoxantrone[43]. In a challenging spontaneous breast cancer model, the combination therapy that provided the most significant therapeutic efficacy also induced the highest level of ICD in cancer cells (Workenhe et al. 2019, manuscript

under review). Studies by other research groups showed that stimulation of TLR4 by HMGB1 released from cancer cells is a key determinant to establishing anti-cancer immune response[23].

Based on these observations, we hypothesize that enhancing TLR4 signalling through virus mediated overexpression of HMGB1 can improve oHSV in the induction of anti-tumor immune response. To test this, we constructed oHSV expressing the HMB C106S mutant, which was shown to stimulate TLR4 signalling during in vitro infection, and evaluated its efficacy in a tolerized breast tumor model.

2. Materials and methods

2.1 Plasmids

pTK-173 (figure 1a) was constructed by inserting HSV-1 thymidine kinase (TK) into pBR322 and described in previous publication[91]. Secretory HMB was designed and synthesized by Samuel T. Workenhe. pTK-Green was constructed by inserting EGFP expression cassette (with CMV promoter and SV40 poly(A) signal) within TK coding sequence of pTK-173. paCAG-mCRT display was a kind gift from Kroemer's Laboratorory[92].

2.2 Immunofluorescence

Cells were seeded onto coverslips and infected at 50% confluence. At indicated times, cells were washed once with PBS and fixed with 10% formalin (Sigma) in PBS; and blocked with IF blocking buffer at 4 °C for 16-24 hr. Cells were washed three times with PBS between each steps. Cells were stained with anti-CRT antibodies (ab2907) diluted in IF blocking buffer for 1 hr at room temperature, then washed three times with PBS, once with IF blocking buffer and probed with anti-mouse or anti-rabbit Alexa Fluor 594-conjugated secondary antibodies 1:500 in IF blocking buffer for 1 hr at room temperature in dark. Nuclei were stained with 1:10,000 Hoechst 33258 dye for 10 min at room temperature in dark. Coverslips were mounted onto microscope slides with IF mounting media. All images were captured with a Leica DM-IRE2 inverted microscope and analyzed using Openlab software (Improvision).

2.3 Restriction Digestions

All restriction endonucleases (SacI, KpnI, AgeI) and corresponding buffers were purchased from New England Biolabs (NEB). Optimal reaction buffers and temperatures for each endonuclease

were used following NEB guidelines . 1 μg/μL DNA samples were mixed with 1U/μL restriction endonucleases and corresponding optimal buffers at 1X concentration. Nuclease free water (Life Technology) was used to dilute all reagents to specified working concentration. All reactions were incubated at optimal temperature for 16hr. To preform digestion using two or more endonuclease with different optimal conditions, digestion products were purified by phenol-chloroform extraction before subjecting to the second restriction endonuclease.

2.4 Ligation

Quick Ligation Kit (NEB M2200L) was used for all ligations. Reactions were prepared at 0 °C as follows: 5 fmol/μL plasmid backbone, and/or 15 fmol/μL insert was mixed in 1X Quick Ligation Reaction buffer (containing 66 mM Tris-HCl, 10 mM MgCl$_2$, 1 mM dithiothreitol, 1 mM ATP, 7.5% polyethylene glycol, pH 7.6 at 25 °C), Quick Ligase (NEB). Nuclease free water (Life Technology) was used to dilute all reagents to specified working concentration. Reaction was incubated at room temperature for 15 min.

2.5 Bacteria

One Shot Stbl3 chemically competent Escherichia coli (Thermo Fisher Scientific C737303) was used in all cloning applications. Cells were stored at -80 °C for long term and thawed at 0 °C before experiment. Cells were cultured in either Lysogeny media (LB) (Sigma-Aldrich), or LB-agar (Bioshop) supplemented with 100 μg/mL Ampicillin (Invitrogen), or 50 μg/mL Kanamycin (Invitrogen). For blue-white screening, LB-Agar plates were supplemented with 100 μg/mL Ampicillin (Invitrogen), 40 μg/mL X-gal (Fermentas), and 50 μg/mL IPTG. Liquid culture was

rocked at 225 rotation per minute (rpm) and LB-Agar plates were incubated at 37 °C overnight to allow growth.

2.6 Transformation

E. coli was transformed following protocol: 10 µL ligation product or 100 pg plasmid was mixed with 50 µL cells, incubated on ice for 30 min, heat-shocked at 42 °C for 45 sec, then on ice for 5 min. 900 µL S.O.C medium (Invitrogen 15544034) was added and rocked at 225 rpm, 37 °C for 1 hr. Cells were then sedimented at 16,000 x g for 1 min, resuspended in 50 µL LB and spread onto 10 cm LB-Agar plate.

2.7 Plasmid Purification

Plasmid from overnight E. coli culture was purified using PureLink HiPure Plasmid Miniprep (Invitrogen K210003) or Midiprep (Invitrogen K210015) kits following the provided protocol 36.

2.8 Agarose Gel Electrophoresis

Agarose (Life Technology) mixed in 1X TAE (including 40 mM Tris, 20 mM Acetic Acid, 1 mM EDTA, pH 8.0) at 1 g:100 mL composition was heated to dissolve. The liquid was allowed to cool and solidified using fixed position combs. Casted agarose gel was placed in agarose gel submarine unit and submerged with 1X TAE buffer.

DNA loading buffer (including 1.67 mM tris-HCl pH 6.7, 0.005% Xylene cyanol, 0.005% OrangeG, 10% glycerol and 10 mM EDTA) was added to DNA sample. 10 µL of each samples were loaded along with 5 µL 1kb + DNA ladder (Invitrogen). Gel was subjected to electrophoresis at 80V for indicated durations. Gels were submerged in ethidium bromide (5

μL/100 mL 1X TAE) with shaking for 15 min and then in water with shaking for 10 min to stain DNA. Signals were visualized under UV transilluminator (AlphaImager).

2.9 Phenol-Chloroform DNA Extraction

DNA samples were mixed thoroughly with equal volume Phenol:Chloroform:Isoamyl Alcohol (25:24:1, v/v) (Invitrogen), and subjected to centrifugation at 14,000 x g at 4 °C for 5 min. Aqueous layer was collected and extraction was repeated twice using Phenol:Chloroform:Isoamyl Alcohol (25:24:1, v/v, Invitrogen) and once with chloroform (Fisher Scientific). 0.1X volume of 5 M sodium acetate and 2X volume of 100% ethanol were added to the samples, incubated at -80 °C for 30 min and DNA was sedimented by centrifugation at 14,000 x g, 4 °C, for 15 min. The DNA pellet was then resuspended in 1X volume of 100% ethanol, sedimented by centrifugation at 14,000 x g, 4 °C for 5 min, and air dried at 37°C.

2.10 Polymerase Chain Reaction (PCR)

Kapa HiFi PCR kit was used for all applications with the exception of site-directed mutagenesis. Reactants were prepared in thin-walled sterile PCR tubes at 0 °C as follows: 1X Kapa HiFi buffer (Kapa Biosystem), 1.2 mM total dNTPs (containing 0.3 mM each of dATP, dCTP, dGTP, dTTP), 0.3 μM specified forward and reverse primer, and 0.05 ng/μL template DNA. Samples were incubated in thermocycler using set conditions as follows: 1) 95 °C for 5 min, 2) 98 °C for 30 sec, 3) optimal annealing temperature for 15 sec, 4) 72 °C for 30 sec/kb, 5) Repeat step 2 to 4 for 29 times, 6) 72 °C for 5 min, 7) hold at 4 °C. PCR products were stored at -20 °C. The lower optimal annealing temperature for the forward and reverse primers were used in the thermocycle.

2.11 DNA Quantification

All DNA samples were quantified using NanoVue Plus Spectrophotometers (GE Healthcare) following provided protocols.

2.12 Whole-cell protein extracts

Cells were washed once with ice-cold PBS and incubated with RIPA buffer supplemented with protease inhibitor cocktail on ice for 10 min, and passed through 30 gauge needle for 5 times. Debris was spin down at 10,000 g for 10 min at 4°C. Supernatant (whole cell protein) was mixed with SDS-loading dye and boiled at 100 °C for 10 min and stored at -20 °C. Protein concentration was quantified using a Bradford kit (Bio-Rad Laboratory).

2.13 Cell culture

Human osteosarcoma cell line (U2OS) was purchased from the American Type Culture Collection (ATCC). Murine breast cancer cells (TUBO) was a kind gift from Dr. Jonathan Bramson. HEK-Blue hTLR4 (InvivoGen) was a kind gift from Dr. Dawn Bowdish. All cells were maintained at 37°C in 5% CO_2 in Dulbecco's modified Eagles medium (DMEM) supplemented with 10% fetal bovine serum, 2mM L-glutamine, and 100U/ml penicillin and streptomycin (P/S, Invitrogen).

2.14 Reagents

HEK-Blue detection media (InvivoGen hb-dec3) was purchased from InvivoGen and prepared as directed. LPS was a kind gift from Dr. Yonghong Wan, it was dissolved in PBS for storage or for detection.

2.15 TLR4 reporter assay

HEK-Blue hTLR4 cells were seeded in 96-well plates at 2E4 cells per well in regular culture media. 24hr after seeding, culture media was replaced with 90μL HEK-Blue detection media and mixed with 10μL of sample for detection. 24hr later, color change of the detection media was measured by absorption at 600nm.

2.16 In vitro infection

U2OS or TUBO cells were seeded at 80% confluency and allowed to settle for 24 hr. Virus was dissolved in DMEM supplemented with 2mM L-glutamine, and 100U/ml penicillin and streptomycin (P/S, Invitrogen) to reach desired multiplicity of infection (MOI). After cells were settled, media was replaced with small volume of dissolved media (1mL for each 10cm dish, scaled according to surface area), and incubated at 37°C in 5% CO_2 with shaking for 1hr. After 1hr, the inoculated virus was replaced with adequate volume of culture media.

2.17 Whole-cell protein extracts

At desired timepoint following infection, culture media was collected (for immune-precipitation) and cells were washed once with ice-cold PBS and incubated with RIPA buffer supplemented with protease inhibitor cocktail on ice for 10 min, and passed through 30 gauge needle for 5 times. Debris was spin down at 10,000 g for 10 min at 4°C. Supernatant (whole cell protein) was mixed with SDS-loading dye and boiled at 100 °C for 10 min and stored at -20°C. Protein concentration was quantified using a Bradford kit (Bio-Rad Laboratory).

2.18 Flag-tag Immuno-precipitation

Culture media collected from infected or transfected cells was filtered through a 0.2µm filter to remove remaining cells. Pierce™ Anti-DYKDDDDK Magnetic Agarose (ThermoFisher Scientific A36797) was directed added to collected media. 50µL of beads (12.5µL bead volume) was added to media collected from a 10cm dish. This mixture was mixed in a 14mL conical tube on an end-to-end rotator at 20 rpm overnight at 4°C. The beads was then sedimented at 1000xg for 5 min. Supernatant was removed, the beads were washed 3X with PBS, and eluded with Glycine pH2.5 for 10 min. The eluded protein was neutralized with Tris to an approximate pH of 7. The sample was then mixed with SDS loading buffer (NEB B7703S) and heated at 95°C for 10 min.

2.19 Mouse Experiments

Mice were maintained at the McMaster University Central Animal Facility with all procedures performed in full compliance with the Canadian Council on Animal Care and approved by the Animal Research Ethics Board of McMaster University. 6- to 7-week-old Balb/c mice (Charles River Laboratory) were used to implant $5x10^5$ TUBO cells subcutaneously on the left flank. To minimize experimental variability, low passage TUBO cells were used for subcutaneous injections. 20-30 days after injection, mice with tumors volume between 50mm^3 and 100mm^3 were treated and the other mice were excluded from experiment. Since tumor sizes are heterogeneous, mice are randomized so that each treatment group has tumors of variable volume at the start of treatment. The tumors were treated by local administration of three 50 µl doses of either PBS or 1×10^7 total pfu oHSV dissolved in PBS, one does each day for three days. Tumors were measured every 3 days, and fold changes in tumor volumes were calculated

relative to the tumor volume at the start of treatment. Mice having tumors exceeding 1000mm^3 were classified as end point. Survival analysis was performed with GraphPad Prism.

3. Results

3.1 Oncolytic HSV-1 did not provide therapeutic efficacy in the MC38 colon carcinoma model

Tumor neoantigens are ideal targets for successful anti-tumor immune responses. To assess whether oncolytic HSV can induce immunity against neoantigens, we planned to use the MC38 colon adenocarcinoma model. Using mass spectrometry in combination with exome sequencing, Yadav et al. identified six neoantigens expressed and presented by MC38[93]. Immunization against three of these neoantigens protected mice against MC38 challenge. The identification of these neoantigens provided a platform to measure the diversity of anti-tumor immunity. To utilize this model for future studies, we verified the ability of oHSV to infect and replicate in MC38. GFP expression and viral production was observed in MC38 infected with d810 (oHSV ICP0-null, GFP-expressing) (Figure 2a, b). Infection by d810 also produced measurable progeny virus (Figure 2c, d). To assess *in vivo* efficacy of oHSV in MC38, we established tumors in C57bl/6 mice and treated them with oHSV (d810) via intratumoral injection. Comparing to PBS treated group, no significant difference was observed in turns of tumor volume or survival (Figure 2e, f). Subsequent in vivo testing of oHSV was preformed on the TUBO breast tumor model based on two considerations. First, emerging data from our colleagues showed induction of T cell response against the MC38-speicific neoantigen, adpgk, failed to protect mice bearing MC38 tumors (Nader El-Sayes 2019, unpublished data). This observation is inconsistent with the published report which indicates adpgk as the immunodominant neoantigen[93]. Therefore, more validation on MC38 neoantigen is needed. Second, previous data suggests oHSV alone can provide partial efficacy in the TUBO model[44], and the efficacy is correlated with ICD markers such as serum HMGB1.

a)

Mock 0.02 0.04 0.08 0.16 0.32

U2OS

0.64 1.28 2.56 5.12 10.24

b)

Mock 0.02 0.04 0.08 0.16 0.32

MC38

0.64 1.28 2.56 5.12 10.24

c) Total Virus Yield (pfu)

d) Burst Size

e)

f)
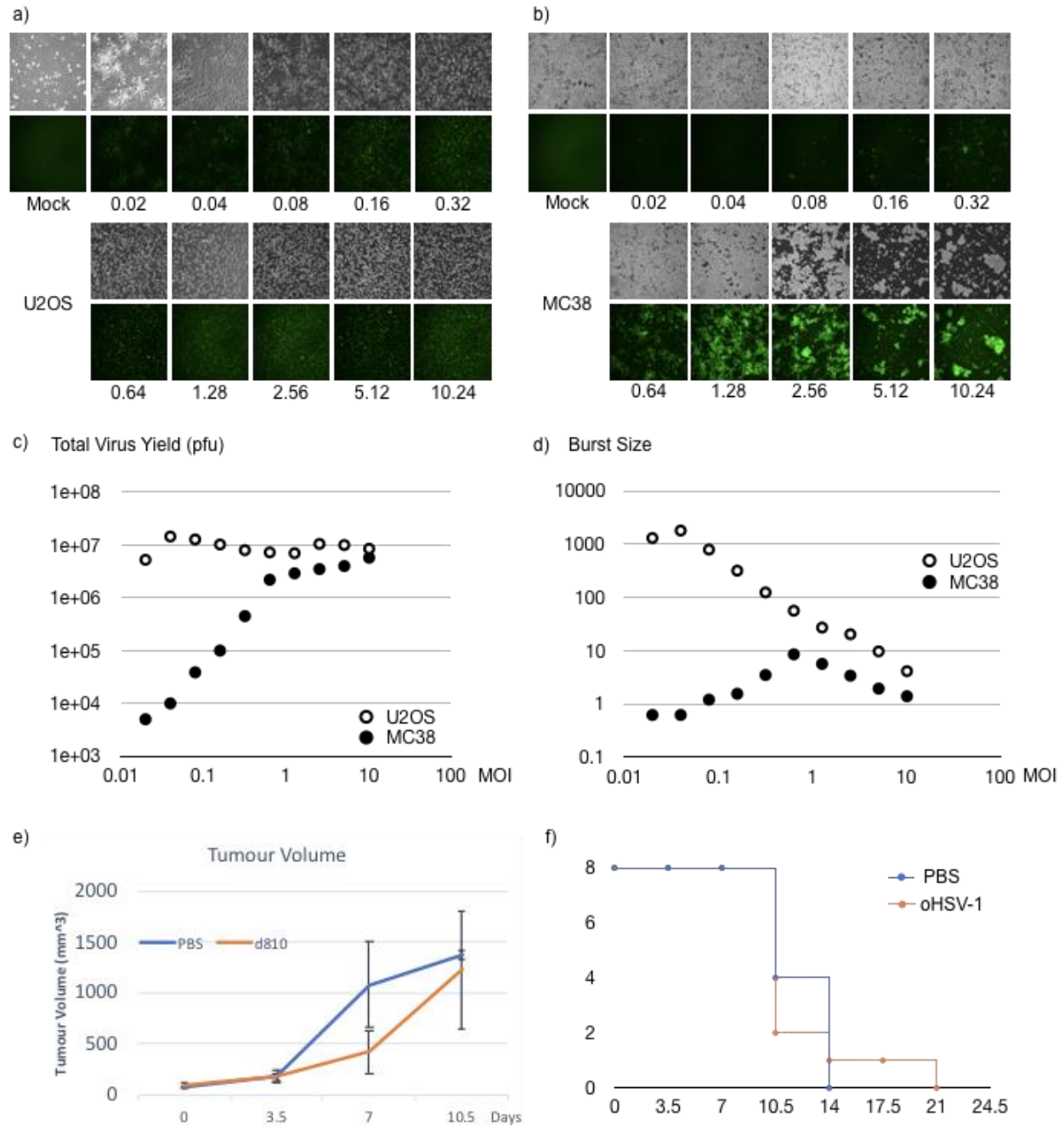
Figure 2: oHSV-1 mono therapy failed to provide therapeutic efficacy in MC38 tumour model. To assess whether oHSV-1 can establish infection in MC38, U2OS and MC38 cells were infected with d810 at indicated MOI for 24 hours. Both cell morphology and GFP signal were observed (a, b). Total virus yield and burst size (calculated as output virus/input virus) were quantified (c, d). To assess the efficacy of oHSV-1 monotherapy in the MC38 model, 2×10^5 MC38 cells were implanted into C57bl6 mice subcutaneously to form tumours. After the tumours reach 50 mm^3, the mice were separated into two groups that have approximately equal average tumour volumes. The tumours were treated with either PBS or 2×10^7 pfu of oHSV-1 (d810) through intratumoural injection. There is no significant difference in mean tumour volume (e) or survival benefit (f).

3.2: Construct homologous donor template to insert the expression cassette of secretory HMGB1 B-box into viral TK gene (UL23)

To build oHSV-1 expressing ecto-CRT or secretory HMGB1 B-box (sHMB), we inserted an expression cassette into the viral genome using homologous recombination (Figure 3). For efficient selection of recombinant virus and minimal impact of insertion on essential viral genes, the site we chose for insertion is within UL23 (Figure 3a). UL23 encodes herpes viral thymidine kinase (TK). TK is involved in generating dNTP to allow viral genome replication in non-proliferating cells. In replicating cells such as cancer cells, dNTP pools are sufficient enough so the role of TK is dispensable, making UL23 a dispensable site for insertional disruption. More importantly, TK phosphorylates acyclovir into acyclovir monophosphate which is subsequently phosphorylated by cellular kinases into acyclovir triphosphate[94]. Acyclovir triphosphate is a highly selective inhibitor of herpes viral DNA polymerase, which disables the replication of TK-competent viruses. Therefore, HSV with TK disruption is resistant to acyclovir. As illustrated in figure 3b, the homologous donor to insert flag-tagged sHMGB1 was made by replacing the EGFP coding sequence in pTK-Green (a plasmid harbouring HSV-1 tk inserted with expression cassette of EGFP). Using immunoblotting (Figure 3c), flag-tagged sHMB was detected in both cellular extract from U2OS cells transfected with pTK-sHMGB1 and in the culture media. No difference in the level of sHMGB1 was observed in the presence of golgi-plug.

Figure 3: Construction of pTK-HMB. a) In pTK-Green, TK was inserted with EGFP expression cassette. CMV pr, CMV promoter; SV40, SV40 poly(A) signal. b) Coding sequence for secretory flag-tagged HMB was amplified with forward and reverse primers with overhangs containing AgeI and KpnI restriction site, respectively. Both pTK-Green and the PCR products were digested with AgeI and KpnI, The purified plasmid backbone and PCR products were ligated to generate pTK-HMGB1 or pTK-CRT. c) To verify the expression and secretion of flag-tagged sHMGB1 B-box from pTK-HMGB1, U2OS cells transfected with pTK-Green and pTK-sHMGB1 was cultured with golgi plug for 24 hours. Protein extract from both the cells and concentrated media was subjected to immunoblot detection of flag-tagged sHMGB1 (predicted size: 13.4kDa). The size of each band corresponding to HMB were approximated using the ladder and GAPDH as reference.

37

3.3: Optimization of recombinant virus selection

To construct recombinant HSV-1 through homologous recombination, HSV-1 infectious DNA was transfected into cells along with a homologous donor. The progeny virus produced from co-transfection was then plaque-purified in acyclovir to select for recombinants. For efficient selection, both the dose of acyclovir and the amount of input virus for acyclovir selection were optimized. To find the concentration of acyclovir that maximally differentiates the growth between non-recombinant and tk-null recombinant virus, U2OS were infected with n212 (a strain of ICP0-null HSV-1 with intact tk) or n212-GFP (with tk disrupted by insertion of EGFP expression cassette, originally created by recombining n212 with pTK-Green) at the multiplicity of infection (MOI) of 1 under different concentrations of acyclovir. 24 hours after infection, the infected cells was collected with culture media and homogenized through freeze-thaw. The viral yield was then quantified in the absence of acyclovir on U2OS cells. At 220μm, acyclovir completely inhibited replication of n212. Replication of n212-GFP in U2OS is unaffected by acyclovir below 200μM, but slightly reduced with higher concentrations of acyclovir (Figure 4a). Besides the concentration of acyclovir, the frequency of finding recombinants also depends on the MOI used for plaque purification. While inputting more virus produced from co-transfection can increase the chance of finding recombinant progeny virus during selection, higher MOI increase the chance that cells infected by recombinant virus is also infected by their wild-type counterparts. Therefore infecting at high MOI during selection limits the plaque formation of recombinant virus as acyclovir monophosphate produced from TK of the wild type virus inhibits replication of recombinant virus as bystander. To optimize the amount of input virus for selection, cells were co-transfected with n212 infectious DNA plus pTK-GFP or pTK-173 as a control. When viruses from co-transfection cause cytopathic effect in 100% of cells, co-

transfected cells were collected and used to infect U2OS cells at MOI of 0.145 and 0.0145, respectively under 100, 200 or 400μM acyclovir (Figure 4b). The frequency of recombinant, GFP-positive plaques peaked at MOI of 0.145 and 100μM acyclovir. To construct oHSV-HMB we transfected U2OS cells with n212 infectious DNA and pTK-HMB. We screened the progeny viruses using the optimized condition for acyclovir-resistant clones. The virus progenies that formed in the presence of acyclovir were isolated and expanded on U2OS cells. To verify the insertion of HMB expression cassette within TK, DNA extracted from the infected cells was subjected to PCR. Amplification using primers annealing within HMGB1 b-box coding sequence produced no signal (figure 5a), while amplification using primers annealing to TK produced products with the same size as wild-type TK (figure 5b), indicating no insertion among the selected virus clones. To find how these virus clones replicate in the presence of acyclovir without insertional disruption in TK, their TK region was sequenced. Shown in figure 5c, these clones all have missense, single nucleotide insertion or deletions in the TK coding sequence that disrupt TK expression. These mutations explained how these non-recombinant virus clones replicate in the presence of acyclovir. This result is also consistent with the observation in figure 4b, where the majority of acyclovir-resistant clones are non-recombinant. To eliminate TK-mutants among infectious viral DNA used for co-transfection, n212 was plaque-purified for 3 rounds. The integrity of TK gene in the purified n212 clones was confirmed with sequencing, and infectious DNA was made from these plaque-purified n212 for co-transfection. Plaque-pure infectious DNA was used for co-transfection, and the acyclovir-resistant plaques were genotyped by PCR. Among the selected 48 acyclovir-resistant plaques, 2 plaques showed signs of insertion by PCR (figure 5d). One plaque was further propagated, its insertion was verified with sequencing and expression of HMGB1 B-box was detected with western blot (figure 5e).

a)

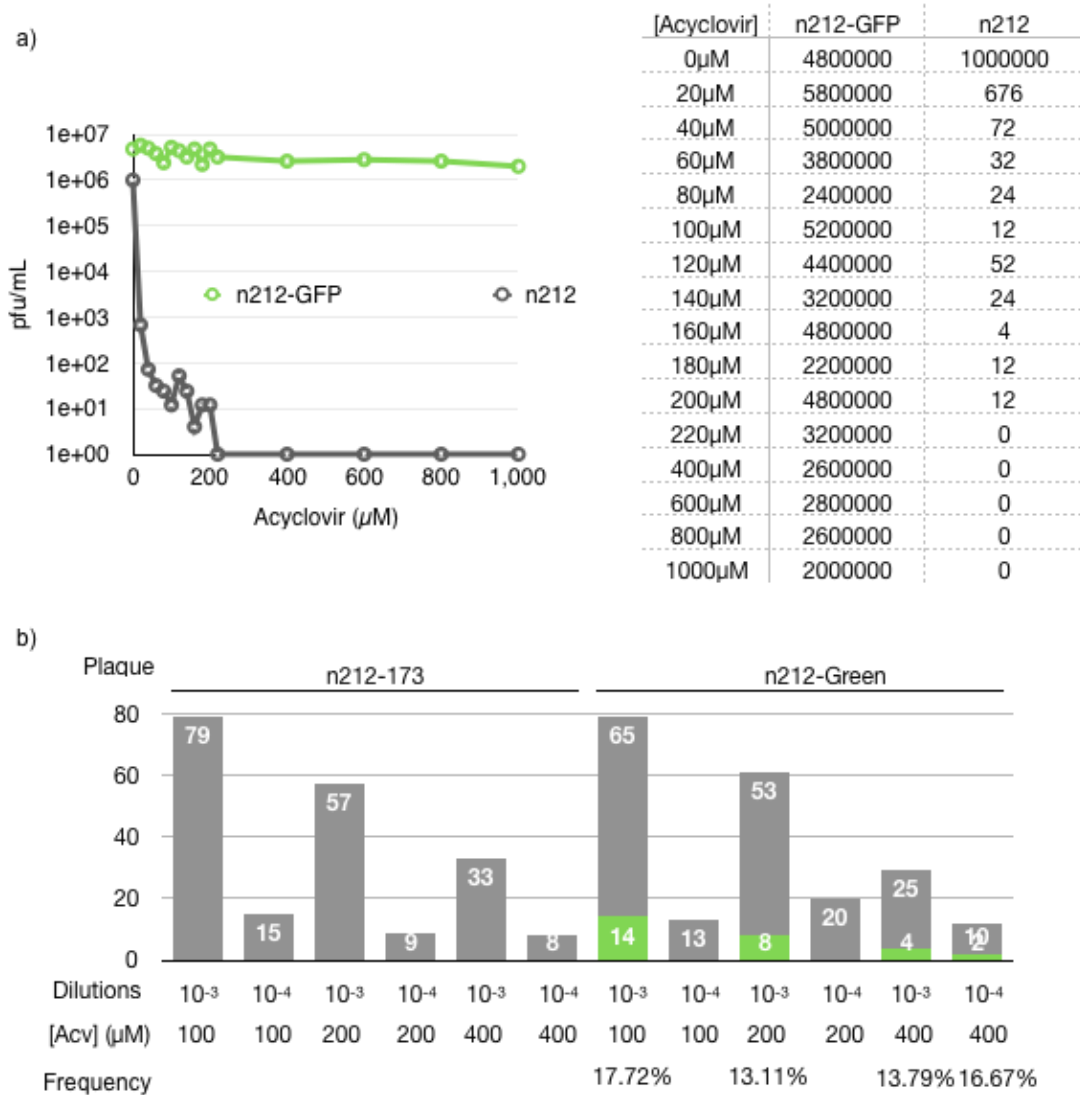| [Acyclovir]	n212-GFP	n212
0µM	4800000	1000000
20µM	5800000	676
40µM	5000000	72
60µM	3800000	32
80µM	2400000	24
100µM	5200000	12
120µM	4400000	52
140µM	3200000	24
160µM	4800000	4
180µM	2200000	12
200µM	4800000	12
220µM	3200000	0
400µM	2600000	0
600µM	2800000	0
800µM	2600000	0
1000µM	2000000	0

b)

Figure 4: Acyclovir dose and input virus optimization. a) To find the concentration range of acyclovir that maximally differentiate the growth between wild-type and tk-null recombinant virus, U2OS were infected with n212 (ICP0-null strain HSV-1 with intact tk) or n212-GFP (with tk disrupted by insertion of EGFP expression cassette) at multiplicity of infection (MOI) of 1 under different concentrations of acyclovir, the viral yield was quantified. b) To compare the amount of input virus and acyclovir dose that can optimally select recombinant virus, co-transfection harvest from n212 with pTK-173 or n212 with pTK-Green was used to infect cells at 10^-3 and 10^-4 dilutions (corresponding to approximate MOI of 0.145 and 0.0145, respectively) under 100, 200 or 400µM acyclovir.
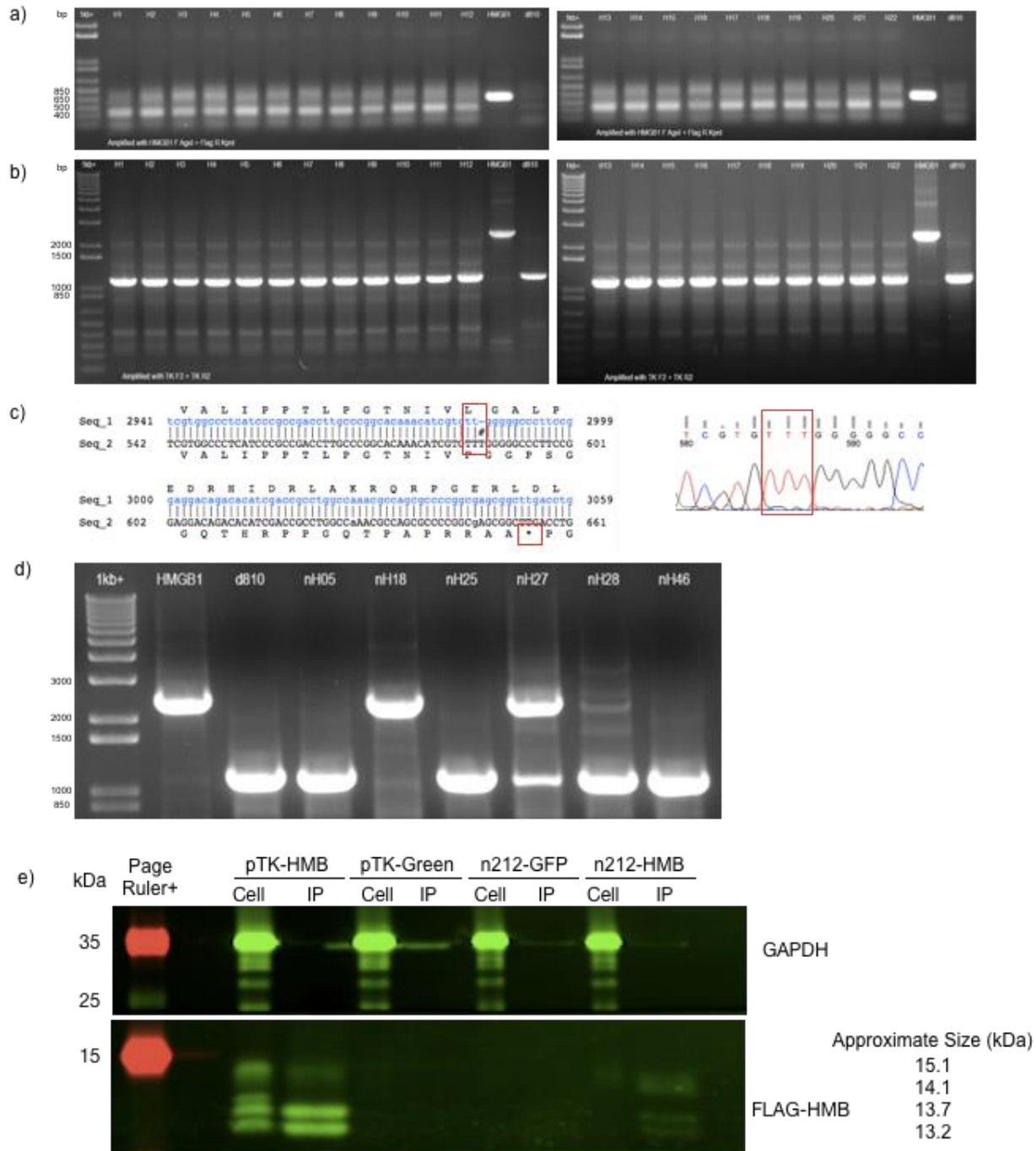
Figure 5: Acyclovir selection of recombinant oHSV-HMGB1 B-box interfered by TK mutation in infectious DNA. Acyclovir-resistant viral progenies generated from HMGB1 co-transfection were expanded by infecting U2OS cells. DNA samples from infected cells were subjected to PCR and resolved on 1% agarose gel. H1-H22: selected acyclovir-resistant clones. HMGB1: positive control using pTK-HMGB1 as template. d810: negative control using HSV-1 dICP0 infected cells as template. a) Amplification of plaque samples using primers annealing within coding sequence of HMGB1 B-box resulted no signal. b) Amplification using primers annealing within TK resulted products with same size as wild-type TK. c) Sequence within TK of these acyclovir-resistant, non-recombinant clones revealed single nucleotide insertion (shown here), deletion or mis-sense mutations that caused pre-mature termination in TK. d) Plaque-purified IVDNA was co-transfected with pTK-HMGB1 B-box and acyclovir-resistant clones were genotyped with PCR. d) Amplification with primers annealing within TK indicated one clone (nH18) is successful recombinant. e) Western blot analysis of U2OS cells transfected with pTK-HMB, pTK-Green, infected with n212-GFP or n212-HMB. Cell: protein extracted from cells. IP: Flag-tagged proteins immunoprecipitated from culture media.

3.4 C106S mutation rescue HMGB1 B-box signalling through TLR4

Early studies indicated that HMB was sufficient to induce macrophage inflammation[95]. The A-box domain alone has no pro-inflammatory activity and can inhibit pro-inflammatory signalling by HMGB1[96]. To test if HMGB1-mediated pro-inflammatory signalling improve oHSV on stimulating anti-tumor immunity, we designed oHSV expressing secretory HMB (sHMB) (Figure 6a). However, culture medium of U2OS transfected with pTK-sHMB did not stimulate TLR4 reporter cells despite the presence of HMB in the medium (Figure 6b, c). More recent studies showed HMBG1 is subjected to various post-translational modifications. Redox states on its three cysteine residues are critical for binding between HMGB1 and TLR4-MD2 complex[97], and B-box alone exhibited low binding affinity towards TLR4-MD2 complex[98]. To verify if our HMB can engage TLR4 signalling, we preformed TLR4 reporter assays on culture media from cells transfected with pTK-sHMB or infected with n212-sHMB. Neither was able to significantly stimulate TLR4 reporter cells (Figure 6b, d). Other studies showed full-length HMGB1 with C106S mutation retain its activity as pro-inflammatory cytokine even in oxidative condition[73]. Synthetic 20-amino acid peptide stretch corresponding to the B-box domain that contains C106S residue significantly stimulates macrophage activation in a TLR4 dependent manner[97]. To circumvent the requirement of redox state for HMB-TLR4 binding, we substituted the cysteine residue in our sHMB to serine using site directed mutagenesis (termed HMB-C106S, as the cysteine residue corresponds to position 106 in full-length HMGB1). Media from cells transfected with pTK-HMB-C106S significantly stimulated TLR4 reporter cells (Figure 6b). Using the same protocol for constructing n212-HMB, we also constructed n212-sHMB C106S. HMB-C106S was detected in infected TUBO cells (Figure 6c). Secreted HMB-C106S was able to stimulate TLR4 reporter cells. (Figure 6d). Among n212-GFP, n212-WT HMB and n212-

HMB C106S, there is no significant difference in cytotoxicity (figure 6e), replication (figure 6f),

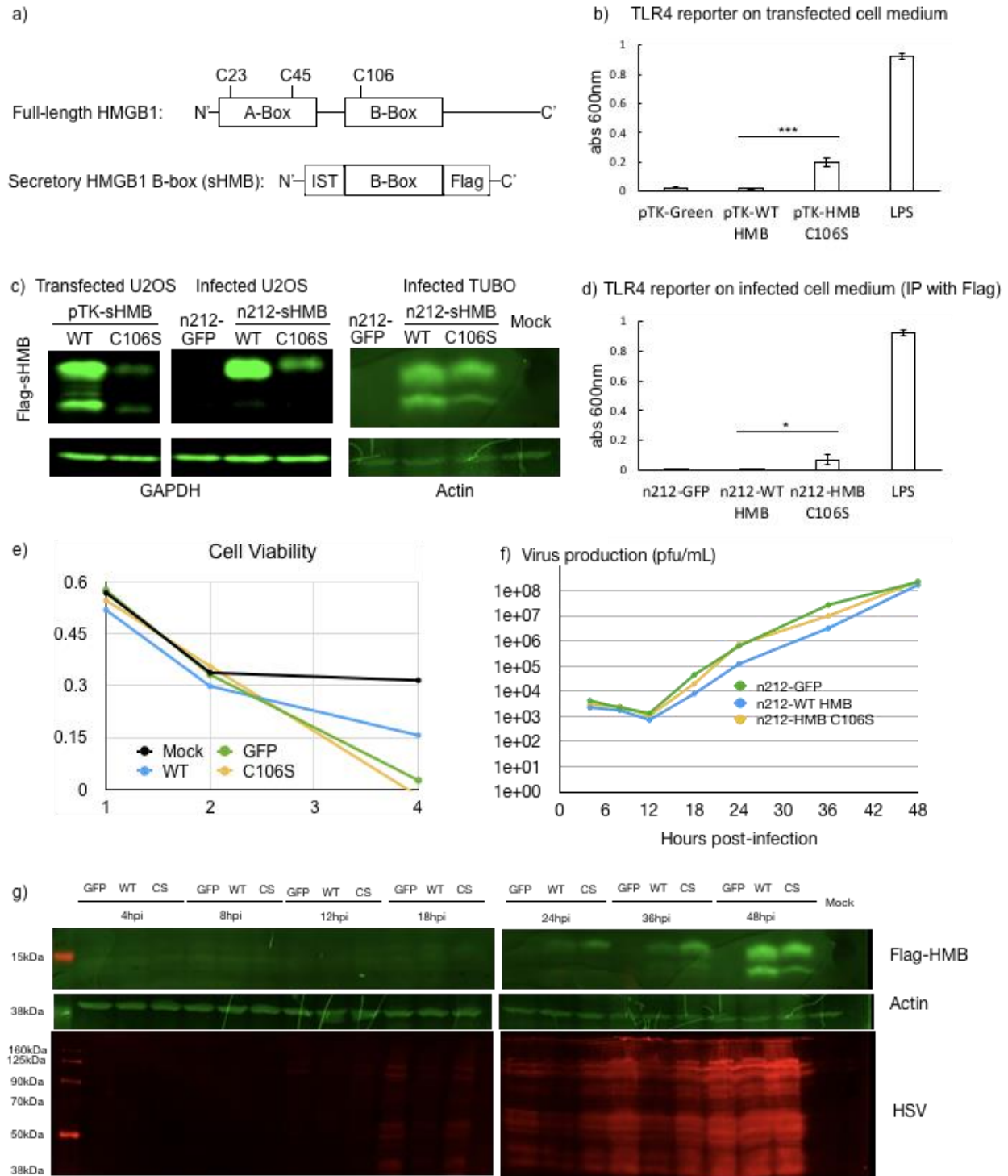and production of other viral proteins (figure 6g).

Figure 6: Construction and characterization of n212-HMB C106S. a) Schematic illustration of sHMB design. IST: human insulin secretion tag; Flag: Flag-tag. b) C106S variant of sHMB stimulates TLR4-MD2 complex. Absorption at 600nm (blanked with absorption of mock-treated cells) reflect TLR4 stimulation. LPS: 2.5ng/mL LPS; other samples: culture media from cells transfected with pTK-GFP, pTK-sHMB, pTK-sHMB C106S. n=3 for each group c) Western blot analysis of U2OS and TUBO cells infected with n212-HMB (WT and C106S variant) d) TLR4 reporter assay on Flag-tagged, immunoprecipitated proteins from infected TUBO cells. n=3 for each group.

3.5 Efficacy of oHSV-HMB in treating breast cancer in a tolerized preclinical model

Next we tested whether the expression of sHMB or its C106S variant can improve therapeutic efficacy of oHSV in a breast cancer. We established tumors in Balb/c mice by transplanting TUBO breast cancer cells, and treated the mice with n212-GFP, n212-WT HMB, or n212-HMB C106S via intratumoral injection. Comparing to mock treatment using PBS control (n=9), treatment with n212-Green (n=7) or n212-WT HMB did not provide significant survival benefit. Treatment with n212-HMB C106S (n=13) provided significant survival benefit compared to PBS treatment, but not compared to the other groups (Figure 7b). 42 days post treatment, five mice bearing small tumors (<200mm^3, 1 treated with n212-GFP, 1 treated with n212-WT HMB, 3 treated with n212-HMB C106S) were re-challenged with a second injection of TUBO cells on their right flank. No secondary tumor was observed for any of these treated mice throughout the experiment (figure 7c). However, relapse from the primary tumors occurred in four of these five re-challenged mice (1 treated with n212-GFP, 1 treated with n212-WT HMB and 2 treated with n212-HMB C106S). These four mice reached endpoint due to relapse by primary tumors.
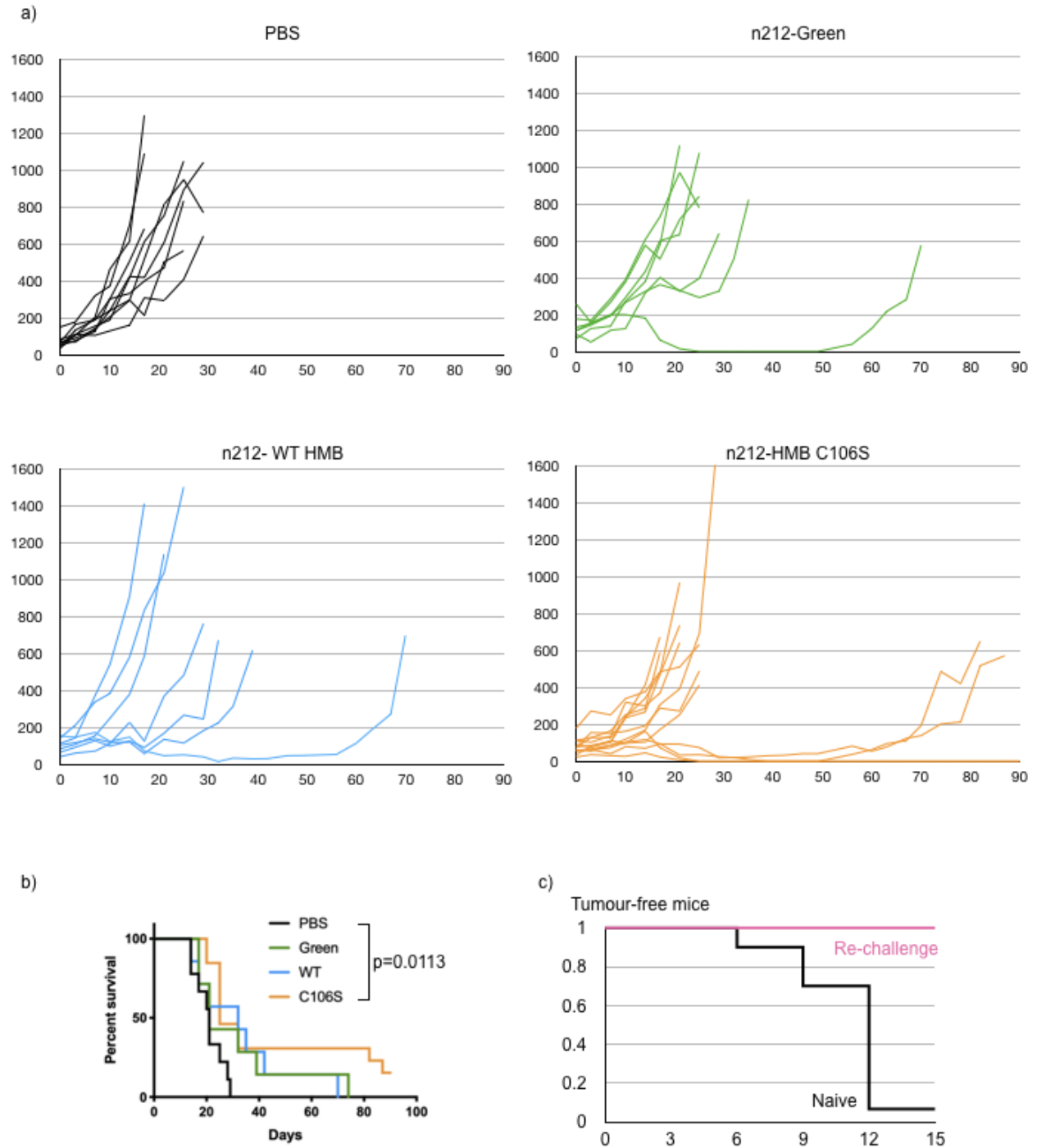
Figure 7: oHSV expressing sHMB C106S provided survival benefit to mice bearing breast tumours. Tumours were established in immunocompetent mice through transplantation of TUBO breast cancer cells. After the tumour reach palpable sizes, they were treated with PBS (n=9), n212-Green (n=7), n212-WT-sHMB (n=7), or n212-sHMB C106S (n=13) through intratumoural injection. a) Tumour volumes for individual mouse. b) Treatment with n212-sHMB C106S significantly extended survival comparing to PBS treatment (p=0.0113). There was no significant difference between other groups. c) 42 days post-treatment, mice bearing small tumours (<200mm³) (n=5 in total) were rechallenged by injecting TUBO cells on the right flank. No tumour was observed on the right flank throughout the experiment.

3.5 Construction of oHSV expressing surface CRT

In addition to HMGB1, another well-characterized hallmark of immunogenic cell death is surface presentation of calreticulin (CRT). CRT on the surface of dying cells or cell fragments is recognized by scavenger receptors on macrophages to initiate phagocytosis, thereby promoting tumor antigen presentation. To test if upregulating CRT surface expression can enhance oncolytic immunotherapy, we planned to construct oHSV expressing surface CRT (figure 8). To enable acyclovir selection of recombinant virus, we inserted the expression cassette of CRT (mCRT-display) within the TK coding sequence of pTK-173 (Figure 8a). This plasmid was named pTK-CRT. Surface presentation of CRT was verified by preforming immunofluorescence analysis with transfected cells without membrane permeabilization. Co-transfection and acyclovir selection were preformed, but no acyclovir-resistant plaques were identified.
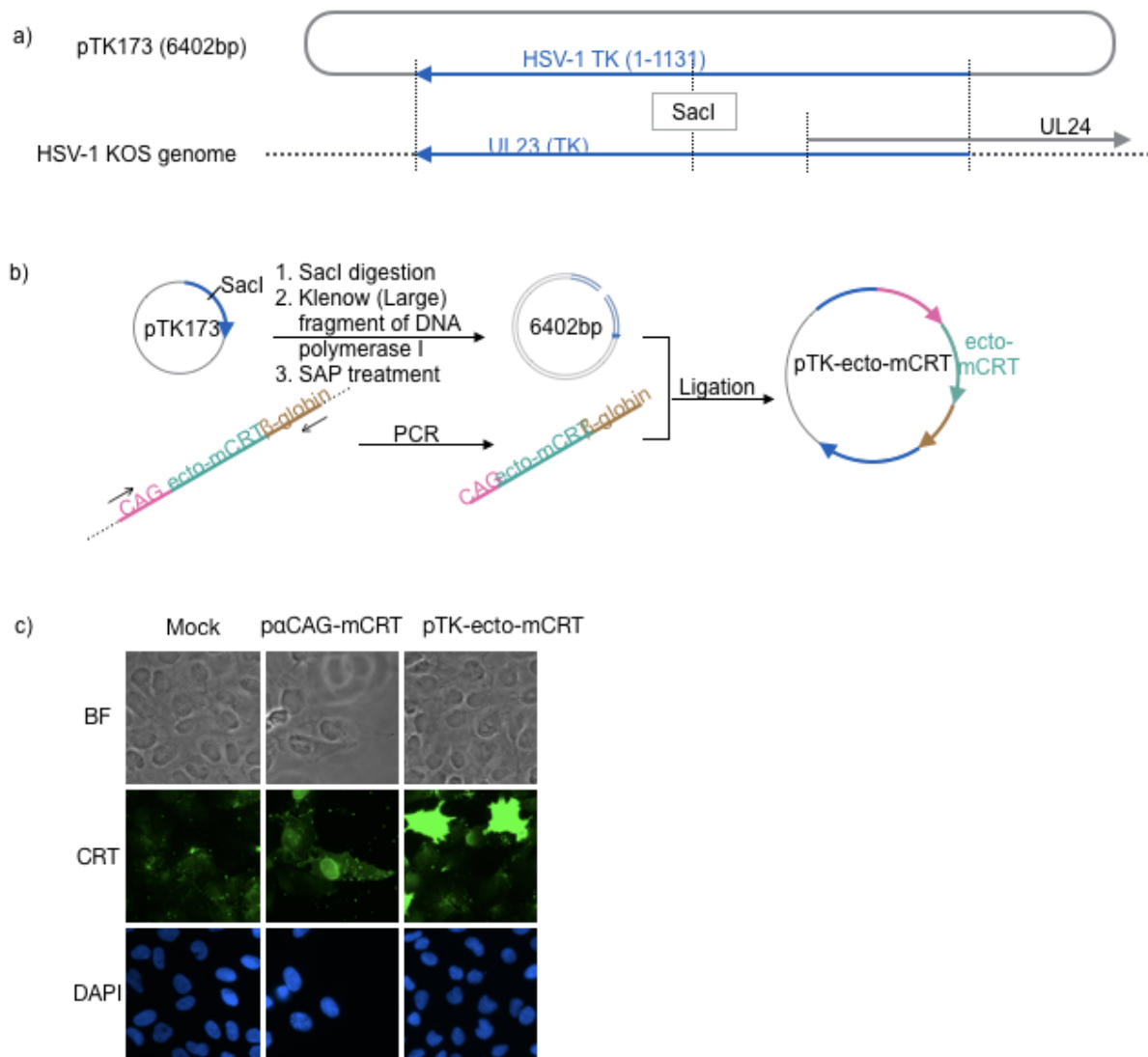
Figure 8: Generation of oHSV-1 expressing surface CRT. a) pTK173 harbours the complete coding sequence of HSV-1 thymidine kinase (TK). b) pTK173 was linearized with SacI, the restriction cut sites were blunted and dephosphorylated with Klenow (large) fragment of DNA polymerase, and shrimp alkaline phosphatase (SAP), respectively. PCR product of the entire mCRT display cassette (with CAG promoter and β-globin poly(A) signal) was ligated into pTK173. Sequence integrity of these constructs were also verified. c) Immunofluorescence microscopy probing mCRT showing surface presentation of mCRT from cells transfected with pTK-ecto-mCRT. Mock: transfected with pTK173 backbone; pαCAG-mCRT: positive control for ecto-CRT used in (ref. 4).

4. Discussion and future directions

4.1 Secretion of B-box from viral infection is suboptimal

Although our recombinant viruses were able to expressed HMB (and its C106S variant) inside infected cells (both TUBO and U2OS), the level of secretion was minimal. As comparison, total WT HMB secreted from 2×10^7 infected U2OS cells was much less than the amount secreted from 1×10^6 transfected U2OS cells (figure 3e). Total HMB C106S secreted by infected TUBO cells stimulated TLR4 reporter cells (figure 4c, d) but was not detectable by western blot (data not shown). These results indicate the secretion of recombinant HMB from viral vectors is not optimal. As there is no evidence of any particular HSV gene product disrupting ER-golgi transportation, the reduced secretion could be a result of overall compromised cellular function during the late phase of infection. HMB expression from infected TUBO cells is not detectable until 24-hour post-infection and high-level expression occurs 48 hours post infection (figure 4g). This delayed expression of HMB from infection is inconsistent with its early expression following transfection, which is detectable at high amounts within 24 hours post-transfection. The HMB expression cassette inserted within TK locus of n212-HMB genome was sequenced and no mutation was detected. Therefore, the CMV promoter in HMB expression cassette may not be suitable for expression from viral vectors. A possible solution is to use the expression cassette used in pCAGGs-mCRT-display. This expression cassette was able to express and secrete a high level of GMCSF from a bovine herpes virus (BHV)-1 recombinant virus (Susan Collins, 2019, unpublished data).

4.2 Potential glycosylation of recombinant B-box

Through western blot analysis (figure 1b, 3e, 4c, 4g), we confirmed the expression and secretion

of recombinant B-box from both plasmid and viral vectors. It is important to point out the size of HMB in these samples varies. Using the migration distance of the standards of the protein ladder and GAPDH as references, HMB in these samples exists in four approximate sizes: 15.1, 14.1, 13.7, and 13.2 kDa. All four size variants of B-box are expressed from plasmid vectors, while only the 13.7 and 13.2 kDa are secreted by transfected cells (figure 1b). U2OS cells infected by n212-HMB (WT or C106S) express predominantly the 15.1 kDa variant (figure 4c), and infected TUBO cells mainly express the 15.1kDa variant and, to a lesser extent, the 13.7kDa variant. The size of HMB predicted from its sequence is 13.4 kDa; there is also an alternative open reading frame that translates to a 12.9 kDa product. The increased sizes of HMB extracted from cells suggest post-translational modifications. In natural settings, HMGB1 is subjected to phosphorylation, acetylation, methylation and/or serine oxidation, which do not result in prominent changes in size. The increased sizes are not a result of ubiquitination as the size increases we observed are all less than a single ubiquitin moiety (8.6kDa). As our HMB contains a human insulin secretion signal, which exports HMB through the ER-Golgi pathway where the majority of N-glycotransferase is localized, this size increase may be a result of glycosylation. Indeed, HMGB1 contains two N-glycosylation sites within the B-box, at N134 and N135. In a study by Kim et al.[99], the size change of HMGB1 by glycosylation is similar to that observed in this study. Glycosylation may also be involved in regulating HMGB1 nuclear export during inflammation, which allows subsequent export. To test if the size increase of B-Box observed is due to glycosylation, the samples containing HMB could be treated with N-deglycosylase before subjecting to western blot.

4.3 Efficacy of n212-HMB C106S in breast tumor require further validations

Comparing to n212-Green or n212-WT HMB, treatment with n212-HMB C106S did not extend survival of mice bearing transplanted breast tumour (figure 5). To answer whether the expression of TLR4-engaging HMB C106S improves oHSV efficacy in breast cancer models, further validation is required. First, we should verify the expression of HMB in tumours treated with n212-HMB (both WT and C106S) and in the serum. In a previous study, the authors observed the release of HMGB1 from TUBO cells infected in vitro by oHSV-2, but not oHSV-1[44]. However, the level of serum HMGB1 in mice bearing TUBO-derived tumours is significantly increased by oHSV-1 infection, not oHSV-2. Therefore, although TUBO cells infected by n212-HMB in vitro secreted low level of HMB (figure 4), this observation may not predict the level of HMB released from in vivo infection. We also need to verify if HMB expressed in vivo can stimulate TLR4. HMB can be subjected to various post-translational modifications but current characterization of HMB functionality is limited to its reduced, unmodified form. To verify if HMB (and its C106S mutant) expressed from in vivo infection can stimulate TLR4 signalling, HMB can be isolated from serum or tumour protein extracts and subjected to TLR4 reporter assay.

4.4 Combination of checkpoint blockade and oHSV-HMB in the MC38 model

oHSV monotherapy provided no therapeutic benefit in the MC38 model (figure7). Triple combination of oHSV, mitomycin C and ICB, however, provided additive which significantly extended survival, controlled tumor volume and induced T cell responses against MC38 neoantigens (Nader El-Sayes, 2019, unpublished data). In both tolerized[43] and spontaneous breast cancer models (Workenhe et al. 2019, manuscript under review), therapeutic efficacy of

oHSV-1 was improved when combined with ICB and chemotherapy that induce tumour ICD. It is possible that the induction of ICD is also the underlying reason for improved response observed in the MC38 model treated with oHSV, ICB combined with mitomycin C. Induction of ICD in tumour can be verified by measuring markers such as serum HMGB1 and HSPs. If ICD does occur in mice treated with triple combination therapy, we can test if the expression of HMB-C106S from oHSV could recapitulate the additive benefit provided by mitomycin C when combined with ICB. Chemotherapies such as mitomycin C and mitoxantrone are not well-tolerized by patients[100,101] and the toxicity towards hematopoietic cells can inhibit the induction of anti-tumour immune response. The advantage of oHSV expressing HMB and other ICD modulators is to replace the chemotherapy therefore avoiding toxicity and complications.

5. Conclusion

Oncolytic viruses are versatile platforms for cancer immunotherapy. However their efficacy in immunologically cold tumors is limited by the abundance of TAAs and various forms of immune evasion within the tumor microenvironment. Previous studies in both tolerized and spontaneous breast cancer models showed that the efficacy of oHSV is correlated to the induction of ICD. Studies by other groups also revealed that engaging TLR4 signalling is essential for establishing anti-tumour immunity. In this study, we demonstrated that the C106S mutant of HMB is a potent stimulator of the TLR4-MD2 complex. oHSV expressing HMB C106S provided marginal therapeutic benefit over parental oHSV or oHSV expressing WT HMB. More studies are needed to test if expression of HMB C106S can improve oHSV. These include detection and function characterization of HMB expressed from oHSV infected tumour, and combining n212-HMB C106S with ICB.

Reference

1. Pardoll, D. M. The blockade of immune checkpoints in cancer immunotherapy. *Nat. Rev. Cancer* **12**, 252–264 (2012).

2. Andtbacka, R. H. I. *et al.* Talimogene Laherparepvec Improves Durable Response Rate in Patients With Advanced Melanoma. *J. Clin. Oncol.* **33**, 2780–2788 (2015).

3. Garon, E. B. *et al.* Pembrolizumab for the Treatment of Non–Small-Cell Lung Cancer. *N. Engl. J. Med.* **372**, 2018–2028 (2015).

4. Brahmer, J. *et al.* Nivolumab versus Docetaxel in Advanced Squamous-Cell Non-Small-Cell Lung Cancer. *N. Engl. J. Med.* **373**, 123–135 (2015).

5. Motzer, R. J. *et al.* Nivolumab for Metastatic Renal Cell Carcinoma: Results of a Randomized Phase II Trial. *J. Clin. Oncol. Off. J. Am. Soc. Clin. Oncol.* **33**, 1430–1437 (2015).

6. Robert, C. *et al.* Pembrolizumab versus Ipilimumab in Advanced Melanoma. *N. Engl. J. Med.* **372**, 2521–2532 (2015).

7. Talimogene Laherparepvec With Pembrolizumab for Recurrent Metastatic Squamous Cell Carcinoma of the Head and Neck (MASTERKEY232 / KEYNOTE-137) - Study Results - ClinicalTrials.gov. Available at: https://clinicaltrials.gov/ct2/show/results/NCT02626000. (Accessed: 22nd August 2019)

8. Talimogene Laherparepvec in Patients With Unresectable Pancreatic Cancer - Study Results - ClinicalTrials.gov. Available at: https://clinicaltrials.gov/ct2/show/results/NCT00402025. (Accessed: 22nd August 2019)

9. Greenman, C. *et al.* Patterns of somatic mutation in human cancer genomes. *Nature* **446**, 153–158 (2007).

10. Samstein, R. M. *et al.* Tumor mutational load predicts survival after immunotherapy across multiple cancer types. *Nat. Genet.* **51**, 202 (2019).

11. Ménard, S., Pupa, S. M., Campiglio, M. & Tagliabue, E. Biologic and therapeutic role of HER2 in cancer. *Oncogene* **22**, 6570 (2003).

12. Downward, J. Targeting RAS signalling pathways in cancer therapy. *Nat. Rev. Cancer* **3**, 11 (2003).

13. Hollstein, M., Sidransky, D., Vogelstein, B. & Harris, C. C. p53 mutations in human cancers. *Science* **253**, 49–53 (1991).

14. Nesbit, C. E., Tersak, J. M. & Prochownik, E. V. MYC oncogenes and human neoplastic disease. *Oncogene* **18**, 3004 (1999).

15. Hellmann, M. D. *et al.* Nivolumab plus Ipilimumab in Lung Cancer with a High Tumor Mutational Burden. *N. Engl. J. Med.* **378**, 2093–2104 (2018).

16. Łuksza, M. *et al.* A neoantigen fitness model predicts tumour response to checkpoint blockade immunotherapy. *Nature* **551**, 517–520 (2017).

17. Dunn, J. & Rao, S. Epigenetics and immunotherapy: The current state of play. *Mol. Immunol.* **87**, 227–239 (2017).

18. Brocks, D. *et al.* DNMT and HDAC inhibitors induce cryptic transcription start sites encoded in long terminal repeats. *Nat. Genet.* **49**, 1052–1060 (2017).

19. Chiappinelli, K. B. *et al.* Inhibiting DNA Methylation Causes an Interferon Response in Cancer via dsRNA Including Endogenous Retroviruses. *Cell* **162**, 974–986 (2015).

20. Merad, M., Sathe, P., Helft, J., Miller, J. & Mortha, A. The Dendritic Cell Lineage: Ontogeny and Function of Dendritic Cells and Their Subsets in the Steady State and the Inflamed Setting. *Annu. Rev. Immunol.* **31**, 563–604 (2013).

21. Kroemer, G., Galluzzi, L., Kepp, O. & Zitvogel, L. Immunogenic Cell Death in Cancer Therapy. *Annu. Rev. Immunol.* **31**, 51–72 (2013).

22. Beavis, Paul. A., Stagg, J., Darcy, P. K. & Smyth, M. J. CD73: a potent suppressor of antitumor immune responses. *Trends Immunol.* **33**, 231–237 (2012).

23. Apetoh, L. *et al.* The interaction between HMGB1 and TLR4 dictates the outcome of anticancer chemotherapy and radiotherapy. *Immunol. Rev.* **220**, 47–59 (2007).

24. Obeid, M. *et al.* Calreticulin exposure dictates the immunogenicity of cancer cell death. *Nat. Med.* **13**, 54 (2007).

25. Slamon, D. J. *et al.* Use of Chemotherapy plus a Monoclonal Antibody against HER2 for Metastatic Breast Cancer That Overexpresses HER2. *N. Engl. J. Med.* **344**, 783–792 (2001).

26. Petrovic, B., Gianni, T., Gatta, V. & Campadelli-Fiume, G. Insertion of a ligand to HER2 in gB retargets HSV tropism and obviates the need for activation of the other entry glycoproteins. *PLOS Pathog.* **13**, e1006352 (2017).

27. Gatta, V., Petrovic, B. & Campadelli-Fiume, G. The Engineering of a Novel Ligand in gH Confers to HSV an Expanded Tropism Independent of gD Activation by Its Receptors. *PLOS Pathog.* **11**, e1004907 (2015).

28. Mamane, Y. *et al.* eIF4E – from translation to transformation. *Oncogene* **23**, 3172–3179 (2004).

29. Lee, C. Y. *et al.* Transcriptional and Translational Dual-regulated Oncolytic Herpes Simplex Virus Type 1 for Targeting Prostate Tumors. *Mol. Ther.* **18**, 929–935 (2010).

30. Kuroda, T., Rabkin, S. D. & Martuza, R. L. Effective Treatment of Tumors with Strong β-Catenin/T-Cell Factor Activity by Transcriptionally Targeted Oncolytic Herpes Simplex Virus Vector. *Cancer Res.* **66**, 10127–10135 (2006).

31. Takeda, K., Kaisho, T. & Akira, S. Toll-Like Receptors. *Annu. Rev. Immunol.* **21**, 335–376 (2003).

32. Ishikawa, H., Ma, Z. & Barber, G. N. STING regulates intracellular DNA-mediated, type I interferon-dependent innate immunity. *Nature* **461**, 788–792 (2009).

33. Kozak, M. & Roizman, B. RNA synthesis in cells infected with herpes simplex virus. IX. Evidence for accumulation of abundant symmetric transcripts in nuclei. *J. Virol.* **15**, 36–40 (1975).

34. Chou, J. & Roizman, B. The gamma 1(34.5) gene of herpes simplex virus 1 precludes neuroblastoma cells from triggering total shutoff of protein synthesis characteristic of programed cell death in neuronal cells. *Proc. Natl. Acad. Sci.* **89**, 3266–3270 (1992).

35. Mundschau, L. J. & Faller, D. V. Endogenous inhibitors of the dsRNA-dependent eIF-2α protein kinase PKR in normal and ras-transformed cells. *Biochimie* **76**, 792–800 (1994).

36. Smith, K. D. *et al.* Activated MEK Suppresses Activation of PKR and Enables Efficient Replication and In Vivo Oncolysis by Δγ134.5 Mutants of Herpes Simplex Virus 1. *J. Virol.* **80**, 1110–1120 (2006).

37. Sistigu, A. *et al.* Cancer cell–autonomous contribution of type I interferon signaling to the efficacy of chemotherapy. *Nat. Med.* **20**, 1301–1309 (2014).

38. Critchley-Thorne, R. J. *et al.* Impaired interferon signaling is a common immune defect in human cancer. *Proc. Natl. Acad. Sci.* **106**, 9010–9015 (2009).

39. Everett, R. D. ICP0, a regulator of herpes simplex virus during lytic and latent infection. *BioEssays* **22**, 761–770 (2000).

40. Lin, R., Noyce, R. S., Collins, S. E., Everett, R. D. & Mossman, K. L. The Herpes Simplex Virus ICP0 RING Finger Domain Inhibits IRF3- and IRF7-Mediated Activation of Interferon-Stimulated Genes. *J. Virol.* **78**, 1675–1684 (2004).

41. Yao, F. & Schaffer, P. A. An activity specified by the osteosarcoma line U2OS can substitute functionally for ICP0, a major regulatory protein of herpes simplex virus type 1. *J. Virol.* **69**, 6249–6258 (1995).

42. Sobol, P. T., Hummel, J. L., Rodrigues, R. M. & Mossman, K. L. PML has a predictive role in tumor cell permissiveness to interferon-sensitive oncolytic viruses. *Gene Ther.* **16**, 1077–1087 (2009).

43. Workenhe, S. T., Pol, J. G., Lichty, B. D., Cummings, D. T. & Mossman, K. L. Combining oncolytic HSV-1 with immunogenic cell death-inducing drug mitoxantrone breaks cancer immune tolerance and improves therapeutic efficacy. *Cancer Immunol. Res.* **1**, 309–319 (2013).

44. Workenhe, S. T. *et al.* Immunogenic HSV-mediated Oncolysis Shapes the Antitumor Immune Response and Contributes to Therapeutic Efficacy. *Mol. Ther.* **22**, 123–131 (2014).

45. Barber, G. N. STING: infection, inflammation and cancer. *Nat. Rev. Immunol.* **15**, 760–770 (2015).

46. Diallo, J.-S. *et al.* A High-throughput Pharmacoviral Approach Identifies Novel Oncolytic Virus Sensitizers. *Mol. Ther.* **18**, 1123–1129 (2010).

47. Dunn, G. P., Koebel, C. M. & Schreiber, R. D. Interferons, immunity and cancer immunoediting. *Nat. Rev. Immunol.* **6**, 836–848 (2006).

48. Chao, M. P. *et al.* Calreticulin Is the Dominant Pro-Phagocytic Signal on Multiple Human Cancers and Is Counterbalanced by CD47. *Sci. Transl. Med.* **2**, 63ra94-63ra94 (2010).

49. Liu, X. *et al.* CD47 blockade triggers T cell–mediated destruction of immunogenic tumors. *Nat. Med.* **21**, 1209–1215 (2015).

50. Elliott, M. R. *et al.* Nucleotides released by apoptotic cells act as a find-me signal to promote phagocytic clearance. *Nature* **461**, 282–286 (2009).

51. Ghiringhelli, F. *et al.* Activation of the NLRP3 inflammasome in dendritic cells induces IL-1β–dependent adaptive immunity against tumors. *Nat. Med.* **15**, 1170–1178 (2009).

52. Martins, I. *et al.* Chemotherapy induces ATP release from tumor cells. *Cell Cycle* **8**, 3723–3728 (2009).

53. Garg, A. D. *et al.* A novel pathway combining calreticulin exposure and ATP secretion in immunogenic cancer cell death. *EMBO J.* **31**, 1062–1079 (2012).

54. Michaud, M. *et al.* Autophagy-Dependent Anticancer Immune Responses Induced by Chemotherapeutic Agents in Mice. *Science* **334**, 1573–1577 (2011).

55. Robson, S. C., Sévigny, J. & Zimmermann, H. The E-NTPDase family of ectonucleotidases: Structure function relationships and pathophysiological significance. *Purinergic Signal.* **2**, 409 (2006).

56. Bustin, M. & Reeves, R. High-mobility-group chromosomal proteins: architectural components that facilitate chromatin function. *Prog. Nucleic Acid Res. Mol. Biol.* **54**, 35–100 (1996).

57. Bonaldi, T., Längst, G., Strohner, R., Becker, P. B. & Bianchi, M. E. The DNA chaperone HMGB1 facilitates ACF/CHRAC-dependent nucleosome sliding. *EMBO J.* **21**, 6865–6873 (2002).

58. Calogero, S. *et al.* The lack of chromosomal protein Hmg1 does not disrupt cell growth but causes lethal hypoglycaemia in newborn mice. *Nat. Genet.* **22**, 276–280 (1999).

59. Kang, R., Zhang, Q., Zeh, H. J., Lotze, M. T. & Tang, D. HMGB1 in Cancer: Good, Bad, or Both? *Clin. Cancer Res.* **19**, 4046–4057 (2013).

60. Polanská, E., Dobšáková, Z., Dvořáčková, M., Fajkus, J. & Štros, M. HMGB1 gene knockout in mouse embryonic fibroblasts results in reduced telomerase activity and telomere dysfunction. *Chromosoma* **121**, 419–431 (2012).

61. Tang, D. *et al.* Endogenous HMGB1 regulates autophagy. *J. Cell Biol.* **190**, 881–892 (2010).

62. Lu, B. *et al.* JAK/STAT1 signaling promotes HMGB1 hyperacetylation and nuclear translocation. *Proc. Natl. Acad. Sci. U. S. A.* **111**, 3068–3073 (2014).

63. Qin, S. *et al.* Role of HMGB1 in apoptosis-mediated sepsis lethality. *J. Exp. Med.* **203**, 1637–1642 (2006).

64. Tsung, A. *et al.* The nuclear factor HMGB1 mediates hepatic injury after murine liver ischemia-reperfusion. *J. Exp. Med.* **201**, 1135–1143 (2005).

65. Wang, H., Yang, H., Czura, C. J., Sama, A. E. & Tracey, K. J. HMGB1 as a Late Mediator of Lethal Systemic Inflammation. *Am. J. Respir. Crit. Care Med.* **164**, 1768–1773 (2001).

66. Yang, H. & Tracey, K. J. Targeting HMGB1 in inflammation. *Biochim. Biophys. Acta BBA - Gene Regul. Mech.* **1799**, 149–156 (2010).

67. Hanahan, D. & Weinberg, R. A. Hallmarks of Cancer: The Next Generation. *Cell* **144**, 646–674 (2011).

68. Yang, H., Antoine, D. J., Andersson, U. & Tracey, K. J. The many faces of HMGB1: molecular structure-functional activity in inflammation, apoptosis, and chemotaxis. *J. Leukoc. Biol.* **93**, 865–873 (2013).

69. Bonaldi, T. *et al.* Monocytic cells hyperacetylate chromatin protein HMGB1 to redirect it towards secretion. *EMBO J.* **22**, 5551–5560 (2003).

70. Ito, I., Fukazawa, J. & Yoshida, M. Post-translational Methylation of High Mobility Group Box 1 (HMGB1) Causes Its Cytoplasmic Localization in Neutrophils. *J. Biol. Chem.* **282**, 16336–16344 (2007).

71. Youn, J. H. & Shin, J.-S. Nucleocytoplasmic Shuttling of HMGB1 Is Regulated by Phosphorylation That Redirects It toward Secretion. *J. Immunol.* **177**, 7889–7897 (2006).

72. Scaffidi, P., Misteli, T. & Bianchi, M. E. Release of chromatin protein HMGB1 by necrotic cells triggers inflammation. *Nature* **418**, 191–195 (2002).

73. Kazama, H. *et al.* Induction of Immunological Tolerance by Apoptotic Cells Requires Caspase-Dependent Oxidation of High-Mobility Group Box-1 Protein. *Immunity* **29**, 21–32 (2008).

74. Chiba, S. *et al.* Tumor-infiltrating DCs suppress nucleic acid–mediated innate immune responses through interactions between the receptor TIM-3 and the alarmin HMGB1. *Nat. Immunol.* **13**, 832–842 (2012).

75. Zhang, W. *et al.* Increased Hmgb1 expression correlates with higher expression of c-iap2 and perk in colorectal cancer. *Medicine (Baltimore)* **98**, (2019).

76. Kusume, A. *et al.* Suppression of Dendritic Cells by HMGB1 Is Associated with Lymph Node Metastasis of Human Colon Cancer. *Pathobiology* **76**, 155–162 (2009).

77. Fuentes, M. K. *et al.* RAGE Activation by S100P in Colon Cancer Stimulates Growth, Migration, and Cell Signaling Pathways. *Dis. Colon Rectum* **50**, 1230–1240 (2007).

78. Xia, W. *et al.* Association of RAGE polymorphisms and cancer risk: a meta-analysis of 27 studies. *Med. Oncol. Northwood Lond. Engl.* **32**, 442 (2015).

79. Sims, G. P., Rowe, D. C., Rietdijk, S. T., Herbst, R. & Coyle, A. J. HMGB1 and RAGE in Inflammation and Cancer. *Annu. Rev. Immunol.* **28**, 367–388 (2010).

80. Sasahira, T., Akama, Y., Fujii, K. & Kuniyasu, H. Expression of receptor for advanced glycation end products and HMGB1/amphoterin in colorectal adenomas. *Virchows Arch.* **446**, 411–415 (2005).

81. Kuniyasu, H. *et al.* Expression of receptors for advanced glycation end-products (RAGE) is closely associated with the invasive and metastatic activity of gastric cancer. *J. Pathol.* **196**, 163–170 (2002).

82. Hofmann, M. A. *et al.* RAGE and arthritis: the G82S polymorphism amplifies the inflammatory response. *Genes Immun.* **3**, 123–135 (2002).

83. Jube, S. *et al.* Cancer Cell Secretion of the DAMP Protein HMGB1 Supports Progression in Malignant Mesothelioma. *Cancer Res.* (2012). doi:10.1158/0008-5472.CAN-11-3481

84. Palumbo, R. *et al.* Src family kinases are necessary for cell migration induced by extracellular HMGB1. *J. Leukoc. Biol.* **86**, 617–623 (2009).

85. Huttunen, H. J., Fages, C. & Rauvala, H. Receptor for Advanced Glycation End Products (RAGE)-mediated Neurite Outgrowth and Activation of NF-κB Require the Cytoplasmic Domain of the Receptor but Different Downstream Signaling Pathways. *J. Biol. Chem.* **274**, 19919–19924 (1999).

86. Huang, C.-Y. *et al.* HMGB1 promotes ERK-mediated mitochondrial Drp1 phosphorylation for chemoresistance through RAGE in colorectal cancer. *Cell Death Dis.* **9**, 1004 (2018).

87. Ivanov, S. *et al.* A novel role for HMGB1 in TLR9-mediated inflammatory responses to CpG-DNA. *Blood* **110**, 1970–1981 (2007).

88. Taguchi, A. *et al.* Blockade of RAGE–amphoterin signalling suppresses tumour growth and metastases. *Nature* **405**, 354–360 (2000).

89. Liang, X. *et al.* Ethyl pyruvate administration inhibits hepatic tumor growth. *J. Leukoc. Biol.* **86**, 599–607 (2009).

90. Hummel, J. L., Safroneeva, E. & Mossman, K. L. The role of ICP0-Null HSV-1 and interferon signaling defects in the effective treatment of breast adenocarcinoma. *Mol. Ther.* **12**, 1101–1110 (2005).

91. Haj-Ahmad, Y. & Graham, F. L. Development of a helper-independent human adenovirus vector and its use in the transfer of the herpes simplex virus thymidine kinase gene. *J. Virol.* **57**, 267–274 (1986).

92. Senovilla, L. *et al.* An Immunosurveillance Mechanism Controls Cancer Cell Ploidy. *Science* **337**, 1678–1684 (2012).

93. Yadav, M. *et al.* Predicting immunogenic tumour mutations by combining mass spectrometry and exome sequencing. *Nature* **515**, 572–576 (2014).

94. Elion, G. B. Mechanism of action and selectivity of acyclovir. *Am. J. Med.* **73**, 7–13 (1982).

95. Li, J. *et al.* Structural Basis for the Proinflammatory Cytokine Activity of High Mobility Group Box 1. *Mol. Med.* **9**, 37–45 (2003).

96. Li, J. *et al.* Recombinant HMGB1 with cytokine-stimulating activity. *J. Immunol. Methods* **289**, 211–223 (2004).

97. Yang, H. *et al.* A critical cysteine is required for HMGB1 binding to Toll-like receptor 4 and activation of macrophage cytokine release. *Proc. Natl. Acad. Sci.* **107**, 11942–11947 (2010).

98. He, M., Bianchi, M. E., Coleman, T. R., Tracey, K. J. & Al-Abed, Y. Exploring the biological functional mechanism of the HMGB1/TLR4/MD-2 complex by surface plasmon resonance. *Mol. Med.* **24**, 21 (2018).

99. Kim, Y. H. *et al.* N-linked glycosylation plays a crucial role in the secretion of HMGB1. *J. Cell Sci.* **129**, 29–38 (2016).

100. Crooke, S. T. & Bradner, W. T. Mitomycin C: a review. *Cancer Treat. Rev.* **3**, 121–139 (1976).

101. Posner, L. E., Dukart, G., Goldberg, J., Bernstein, T. & Cartwright, K. Mitoxantrone: an overview of safety and toxicity. *Invest. New Drugs* **3**, 123–132 (1985).